LETTER

doi:10.1038/nature26141

Optogenetic regulation of engineered cellular metabolism for microbial chemical production

Evan M. Zhao[1], Yanfei Zhang[1], Justin Mehl[1], Helen Park[1], Makoto A. Lalwani[1], Jared E. Toettcher[2] & José L. Avalos[1,3]

The optimization of engineered metabolic pathways requires careful control over the levels and timing of metabolic enzyme expression[1–4]. Optogenetic tools are ideal for achieving such precise control, as light can be applied and removed instantly without complex media changes. Here we show that light-controlled transcription can be used to enhance the biosynthesis of valuable products in engineered *Saccharomyces cerevisiae*. We introduce new optogenetic circuits to shift cells from a light-induced growth phase to a darkness-induced production phase, which allows us to control fermentation with only light. Furthermore, optogenetic control of engineered pathways enables a new mode of bioreactor operation using periodic light pulses to tune enzyme expression during the production phase of fermentation to increase yields. Using these advances, we control the mitochondrial isobutanol pathway to produce up to $8.49 \pm 0.31\ g\,l^{-1}$ of isobutanol and $2.38 \pm 0.06\ g\,l^{-1}$ of 2-methyl-1-butanol micro-aerobically from glucose. These results make a compelling case for the application of optogenetics to metabolic engineering for the production of valuable products.

Metabolic engineering aims to rewire the metabolism of organisms for efficient conversion of inexpensive substrates into valuable products such as chemicals, fuels, or drugs[1,2]. Fine-tuning the timing and levels of expression of enzymes involved in both natural and engineered pathways can relieve bottlenecks and minimize the metabolic burden of chemical production[3,4]. This is especially critical when the product of interest or its precursors are toxic, or when the biosynthetic pathway of interest competes with endogenous pathways that are essential for cell growth.

To address these challenges, metabolic engineers frequently use inducible systems to control metabolic enzyme expression[5–7] (see Supplementary Discussion). This approach makes it possible to separate bioreactor operation into two phases: a growth phase, during which product biosynthesis is repressed, and a production phase, when flux through the engineered pathway is maximized. Essential pathways that compete with product formation can be controlled with 'metabolic valves'—genetic programs that express essential enzymes during the growth phase to build biomass, and repress them during the production phase to redirect metabolism towards desired products[5,8].

Light is an attractive strategy to control gene expression in yeast for metabolic engineering applications. It is inexpensive and compatible with any carbon source or nutrient composition. Furthermore, light can be applied or removed instantaneously; this precise control over the level or duration of enzyme expression could simplify the screening of optimal proportions of metabolic pathway enzymes and enable new time-varying modes of control[9,10]. Light-switchable transcription modules have been shown to enable non-toxic, tunable gene expression in a variety of organisms[11,12], including yeast[11,13–15]. We thus sought to test whether optogenetics could be used to control rewired cellular metabolisms to overproduce valuable chemicals.

Here, we describe two powerful optogenetic gene expression systems for yeast, OptoEXP and OptoINVRT, based on the blue light-activated EL222 gene expression system[12]. Using these systems, we show that it is possible to activate and to repress distinct sets of genes in a light-dependent manner. We apply our approach to control endogenous and engineered metabolic pathways to define the growth and production phases of fermentation, enabling production of three valuable chemicals (lactate, isobutanol and 2-methyl-1-butanol (2-MBOH)), the biosyntheses of which directly compete with essential ethanol production. Using a time-varying illumination schedule, we achieve titres of $8.49 \pm 0.31\ g\,l^{-1}$ (mean ± s.d.) of isobutanol and $2.38 \pm 0.06\ g\,l^{-1}$ of 2-MBOH. Our results thus reveal that a simple technology—bidirectional light-controlled enzyme expression—offers a rich set of tools for metabolic engineering.

Our first goal was to construct bidirectional gene circuits in yeast to either induce or repress genes of interest with light. We used the EL222 optogenetic transcription system, which consists of a light-sensitive transcription factor from *Erythrobacter litoralis* (EL222) and its corresponding C120 promoter (P_{C120}), to drive the expression of a gene of interest[16–18] (Fig. 1a). The EL222 system is a robust and versatile gene expression platform, previously applied in *Escherichia coli*, mammalian cells and zebrafish[12,19,20]. We first constructed a yeast strain, YEZ139, in which expression of VP16–EL222 (a fusion of EL222 with the transcriptional activation domain of VP16 and a nuclear localization signal) was driven by the strong constitutive promoter of *PGK1* (P_{PGK1}) (P_{PGK1}–VP16–EL222) and expression of green fluorescent protein (GFP) was driven by the P_{C120} promoter (P_{C120}–GFP; see Methods, Supplementary Tables 1, 2, Extended Data Fig. 1). We called this system (and variants with different promoters driving EL222) OptoEXP.

OptoEXP enables strong and titratable light-inducible gene expression. In both glucose and glycerol media, cells with OptoEXP controlling GFP expression show a 43-fold increase in GFP expression when exposed to constant light compared to cells incubated in the dark, whereas intermittent light pulses produce intermediate expression levels (Fig. 1b, Extended Data Fig. 2). We found that all light sources used were sufficiently bright to activate the EL222 system maximally; thus, varying duty cycle was a reliable and reproducible method for achieving intermediate gene expression output (Extended Data Fig. 3, Methods). The maximum activation levels of OptoEXP are comparable to those reached by the *ADH1* promoter (P_{ADH1}), a constitutive promoter commonly used in metabolic engineering (Fig. 1c).

To construct a light-repressible gene circuit, we inverted the response of the OptoEXP system in a manner akin to the NOT logic gate used in digital processes. We harnessed the yeast galactose (GAL) regulon[21], in which Gal80 binds to and inhibits the Gal4 transcription factor, blocking its ability to induce expression from the *GAL1* promoter (P_{GAL1}). We reasoned that engineering yeast cells with constitutive expression of *GAL4* and *GAL80* expression under the control of VP16–EL222 would lead to constitutive expression from

[1]Department of Chemical and Biological Engineering, Hoyt Laboratory, Princeton University, 25 William Street, Princeton, New Jersey 08544, USA. [2]Department of Molecular Biology, 140 Lewis Thomas Laboratory, Washington Road, Princeton, New Jersey 08544, USA. [3]The Andlinger Center for Energy and the Environment, Princeton University, 86 Olden Street, Princeton, New Jersey 08544, USA.

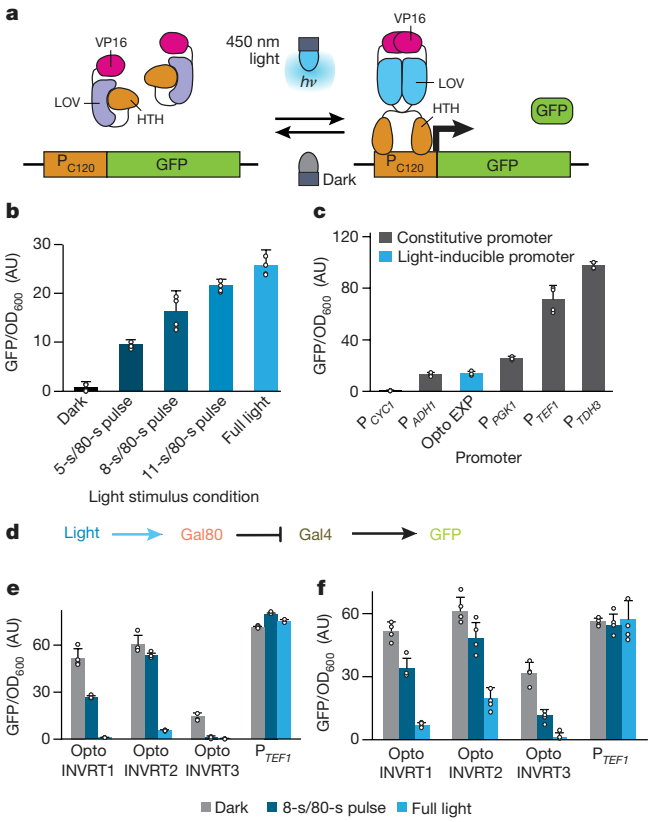

Figure 1 | Characterization of optogenetic circuits. a, Reversible OptoEXP system based on VP16–EL222 that is sensitive to 450 nm light. $h\nu$ indicates the energy of photons. HTH, helix–turn–helix DNA-binding domain. **b**, GFP expression with OptoEXP (YEZ139) tuned with different duty cycles, for example 5-s/80-s pulse means that the light was on for 5 s and off for 75 s. AU, arbitrary units of fluorescence and optical density. **c**, Maximum GFP expression from OptoEXP compared to common constitutive promoters using strains YEZ27 (*CYC1* promoter, P_{CYC1}), YEZ28 (P_{ADH1}), YEZ29 (P_{PGK1}), YEZ30 (P_{TDH3}), YEZ31 (P_{TEF1}) and YEZ32 (P_{C120}). **d**, OptoINVRT circuit diagram (details in Extended Data Fig. 4a, b). **e**, OptoINVRT circuits in CENPK.2-1C-derived (*GAL80*Δ, *GAL4*Δ) strains YEZ100 (OptoINVRT1), YEZ101 (OptoINVRT2) and YEZ102 (OptoINVRT3). **f**, OptoINVRT circuits in BY4741-derived (*GAL80*Δ, *PDC1*Δ, *PDC5*Δ, *PDC6*Δ) strains YEZ115 (OptoINVRT1), YEZ116 (OptoINVRT2) and YEZ117 (OptoINVRT3). All data are shown as mean values; dots represent individual data points; error bars represent the s.d. of four biologically independent 1-ml sample replicates exposed to the same conditions. All experiments were repeated at least three times.

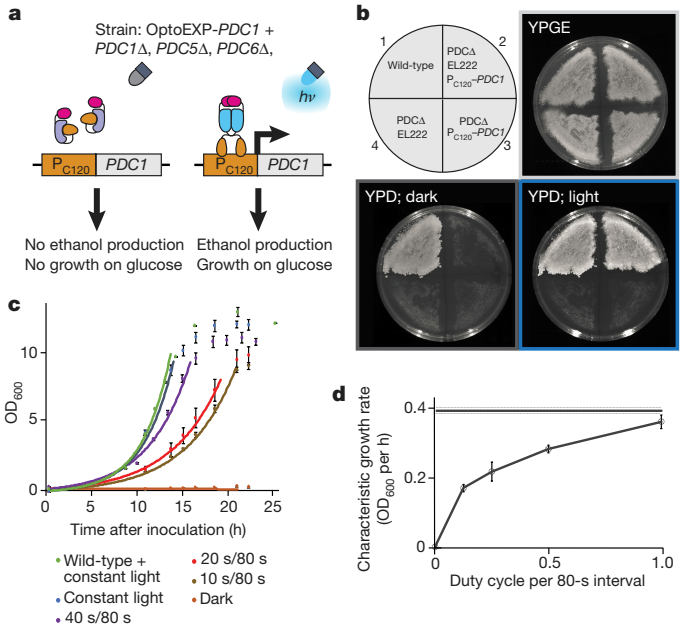

Figure 2 | A light-dependent metabolic valve for ethanol production. a, Using OptoEXP to build light-inducible metabolic valve for *PDC1*. **b**, Light-dependent growth on glucose of a triple PDC mutant strain containing the OptoEXP-*PDC1* metabolic valve. Top left, wild-type BY4741; top right, YEZ61-23 (*PDC1*Δ, *PDC5*Δ, *PDC6*Δ, P_{TEF1}–VP16–EL222, P_{C120}–*PDC1*); bottom left, YEZ50C (*PDC1*Δ, *PDC5*Δ, *PDC6*Δ, P_{TEF1}–VP16–EL222); bottom right, YEZ61C (*PDC1*Δ, *PDC5*Δ, *PDC6*Δ, P_{C120}–*PDC1*). **c**, YEZ61-23 and BY4741 growth in liquid synthetic complete medium supplemented with 2% glucose at different light doses, with best fits to exponential growth curves. **d**, Maximum growth rate of YEZ61-23 as a function of light. Solid line represents the mean wild-type (BY4741) growth rate (dotted lines indicate the s.d.). All data are shown as mean values (values for individual points are available in the Source Data for this figure); error bars represent the s.d. of three biological replicates exposed to the same conditions. All experiments were repeated at least three times.

the P_{GAL1} promoter in the dark and repression of P_{GAL1} in the light (Fig. 1d, Extended Data Fig. 4a, b).

Starting from a strain in which both *GAL80* and *GAL4* are deleted, YEZ44, we constructed three variants of this core inverter topology, which we termed OptoINVRT1, OptoINVRT2 and OptoINVRT3 (Supplementary Tables 1, 2). These variants differed in the strength of the promoter driving *GAL4* and the fusion of a photosensitive degron (PSD) domain[22] to the C terminus of Gal4 to induce faster and more complete light-dependent repression (Extended Data Fig. 4a, b and Supplementary Table 3). Using P_{GAL1}–GFP as a reporter, we found that all three OptoINVRT circuits exhibit robust light-induced gene repression (Fig. 1e, Supplementary Table 4). OptoINVRT2 has the highest maximum expression in the dark (in YEZ101, almost 85% of *TEF1* promoter (P_{TEF1}) levels), while OptoINVRT3 has the highest levels of repression (in YEZ102, more than 70-fold) and lowest expression in full light. All three OptoINVRT circuits show similar responses in a second yeast strain, Y202, which is relevant for metabolic engineering owing to the deletion of all three of its pyruvate decarboxylase genes (strain S288C with the following mutations: *GAL80*Δ, *PDC1*Δ, *PDC5*Δ and *PDC6*Δ) (Fig. 1f, Supplementary Table 4). Our results thus demonstrate that the OptoINVRT platform can achieve a wide range of expression levels, light sensitivities and fold-change responses in different strain backgrounds for flexible incorporation in diverse metabolic engineering applications.

To reduce the ethanol by-product in pyruvate-derived chemical biosyntheses, while still allowing cell growth on glucose, we used OptoEXP to control pyruvate decarboxylation (PDC), an essential step in ethanol biosynthesis. Completely removing PDC activity in *S. cerevisiae* (by deleting *PDC1*, *PDC5* and *PDC6*) does not suffice, because the triple deletion renders yeast unable to grow on glucose owing to the essential role of these genes in NAD^+ recycling for glycolysis[23] and to the lack of effective alternatives for ATP generation owing to glucose-mediated repression of respiration[24]. Thus, we used our OptoEXP circuit to build a light-dependent metabolic valve for *PDC1* expression (Fig. 2a). Light stimulation 'opens' the valve, enabling robust cell growth and ethanol production; dark incubation 'closes' the valve to limit the metabolism of pyruvate into ethanol, thereby inhibiting cell growth on glucose, and enhancing the biosynthesis of alternative pyruvate-derived products.

A strain with all PDC genes deleted and with OptoEXP driving *PDC1* expression, YEZ61-23 (Supplementary Table 2), exhibits light-dependent growth on glucose. YEZ61-23 grows on glycerol with ethanol (yeast peptone with 3% glycerol and 2% ethanol (YPGE)) independently of light because PDC is dispensable for respiration. However, it is only able to grow on glucose plates (yeast peptone with 2% glucose (YPD)) in the presence of blue light (Fig. 2b), with

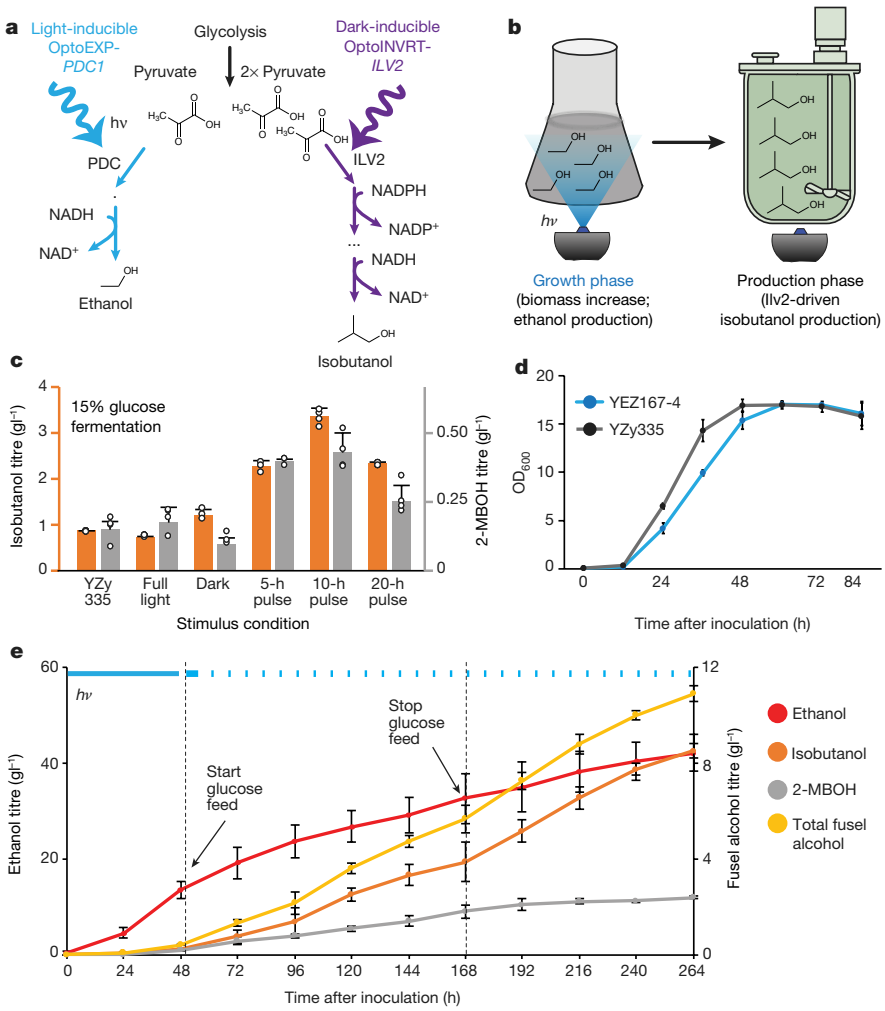

Figure 3 | Light-controlled isobutanol production. a, Ethanol and isobutanol biosynthesis controlled by OptoINVRT-*ILV2* and OptoEXP-*PDC1*, respectively. **b**, Blue light allows growth of YEZ167-4 in glucose, as well as ethanol formation, whereas dark conditions initiate the production phase by stopping *PDC1* induction and de-repressing *ILV2*. **c**, Isobutanol and 2-MBOH production of YEZ167-4 in fermentations of 80 h in 150 g l^{-1} glucose and blue light pulses of 15 s on and 65 s off for 30 min every 5, 10, or 20 h. YZy335 is a light-insensitive isobutanol-producing control strain. **d**, Growth of YEZ167-4 in a 2-l bioreactor and under constant blue light, compared to the YZy335 light-insensitive control. **e**, Isobutanol and 2-MBOH production of YEZ167-4 in a 0.5-l fed-batch pH-controlled fermenter using periodic light stimulation during the production phase. Total fusel alcohols represent the sum of isobutanol and 2-MBOH. Blue bar indicates the time of blue light exposure. Dotted lines indicate the start and stop of the glucose feed. All data are shown as mean values; dots in **c** represent individual data points; individual points for **d** and **e** are available in the Source Data for this figure and Supplementary Table 5, respectively; error bars represent the s.d. of three biological replicates (**c**) or three separate bioreactor runs (**d**, **e**). All experiments were repeated at least twice.

its growth rate in liquid medium reaching 91.9 ± 4.9% of the wild type (BY4741) at full light (Fig. 2c, d). Substantial growth is achieved even at low light doses (43.7 ± 2.7% of wild-type growth rate with only 12.5% light duty cycle), suggesting that light-dependent growth may be achieved at cell densities relevant for metabolic engineering applications.

We then tested whether the bidirectional control afforded by combining our OptoEXP and OptoINVRT circuits could be used to drive two phases of cellular metabolism: a growth phase with mainly ethanol fermentation and a production phase in which carbon accumulates as a desired valuable product instead (either lactate or isobutanol). Production of lactate or isobutanol competes directly with ethanol production as distinct enzymes modify pyruvate to produce each product (pyruvate decarboxylase 1 (Pdc1) in the case of ethanol, lactate dehydrogenase (Ldh) in the case of lactate, and acetolactate synthase (Ilv2) and subsequent enzymes in the case of isobutanol) (Fig. 3a, Extended Data Fig. 5a). We reasoned that by controlling the expression of *PDC1* with OptoEXP and the expression of Ldh or *ILV2* with OptoINVRT, moving cells from light to dark would shift the metabolism from the production of ethanol to the production of lactate or isobutanol (Fig. 3b, Extended Data Fig. 5b).

We first tested our strategy in the simpler case of lactate biosynthesis, which requires overexpression of only one enzyme (Ldh). The presence of lactate is also is well tolerated by yeast. We integrated multiple copies of P_{GAL1}–Ldh and P_{C120}–*PDC1* into our Y202-derived OptoINVRT strains (Extended Data Fig. 6a) and observed a pronounced increase in lactate biosynthesis upon a shift from dark to light, consistent with light-dependent changes in *PDC1* and Ldh expression levels (Methods, Extended Data Figs 4c, 5). On the basis of these results, we next tested our optogenetic circuits on the more complex biosynthesis of isobutanol (Fig. 3a, b), an advanced biofuel with much higher toxicity than lactate. Our approach was to optogenetically control only the first enzyme in the isobutanol pathway (acetolactate synthase), reasoning that if subsequent enzymes were constitutively expressed, the overall pathway flux would still be light-controlled.

We transformed Y202 with OptoEXP, each one of the OptoINVRT circuits, multiple copies of P_{GAL1}–*ILV2* and P_{C120}–*PDC1* and the rest of the mitochondrial isobutanol biosynthetic pathway under strong

constitutive promoters[25], to produce strains YEZ159, YEZ156 and HPY6 (Supplementary Tables 1, 2, Methods). We found that colonies from YEZ159, containing OptoINVRT1, produced the highest isobutanol titres from 4% glucose (Extended Data Fig. 4d, e). To enhance isobutanol production further, we deleted the mitochondrial branched chain amino acid aminotransferase (encoded by *BAT1*, also known as *YBT1*), which competes for the α-ketoisovalerate precursor[26,27], resulting in strain YEZ167-4 (Supplementary Table 2). YEZ167-4 contains six copies of P_{C120}–*PDC1* (Extended Data Fig. 6a), leading to fast cell growth under full light.

By varying the cell density at which cultures are switched from dark to light and the incubation time in the dark before starting the fermentation (Extended Data Fig. 5c), we found that YEZ167-4 can produce as much as $735 \pm 15\,mg\,l^{-1}$ of isobutanol from 2% glucose over 48 h (a yield of 34.2 ± 0.7 mg isobutanol g^{-1} glucose, Extended Data Fig. 7). Switching to 15% glucose and fermentation periods of 80 h only increases production to $1.22 \pm 0.11\,g\,l^{-1}$ of isobutanol (Fig. 3c). However, under these conditions YEZ167-4 is unable to consume all the glucose in the medium (Extended Data Fig. 8a), indicating a stalled fermentation in which cells have undergone premature metabolic arrest.

We hypothesized that during prolonged dark incubation, Pdc1 becomes limiting to a point at which cellular metabolism arrests owing to NAD^+ depletion. We reasoned that periodic pulses of light during the production phase of fermentation could transiently induce *PDC1* expression, thus increasing NAD^+ pools and restoring cellular metabolism, glucose consumption and isobutanol production. We tested different light schedules, applying periodic illumination bouts (30 min of blue light at a duty cycle of 15 s on and 65 s off once every 5, 10 or 20 h throughout the production phase of the fermentation, which lasted 80 h). When cells are exposed to one light bout every 10 h, isobutanol production nearly triples to $3.37 \pm 0.17\,g\,l^{-1}$ (Fig. 3c), and 2-MBOH, another desirable advanced biofuel co-produced with the mitochondrial isobutanol pathway[25], is produced at $433 \pm 69\,mg\,l^{-1}$. These isobutanol yields are more than 2.5 times higher than if cells are kept in the dark throughout the production phase of the fermentation, and four times higher than YZy335, a strain that contains the entire isobutanol pathway and *BAT1* deletion but lacks light-inducible metabolic control. We directly confirmed that our light pulses partially replenish the NAD^+ metabolite pool under these fermentation conditions (Methods, Extended Data Fig. 8b).

To determine the applicability of optogenetics to metabolic engineering in laboratory-scale bioreactors, we measured the growth of the OptoEXP-driven *PDC1* strain, YEZ167-4, in a 2-l fermenter with 15% glucose and constant blue light (Extended Data Fig. 9a, b). Under these conditions, YEZ167-4 is able to reach the same optical density at 600 nm ($OD_{600} = 17.1$) as a light-independent, PDC^+ strain, YZy335 (Supplementary Table 2), indicating that light penetration into the bioreactor is sufficient to drive robust *PDC1* expression and growth (Fig. 3d). We then measured the production of isobutanol and 2-MBOH in fed-batch 0.5-l bioreactors under microaerobic conditions and pH control (Extended Data Fig. 9c, d). We used constant illumination to build YEZ167-4 biomass during a batch growth phase, and then switched to a fed-batch production phase with periodic bouts of light to maintain sufficient NAD^+ levels to preserve metabolic activity. This fermentation strategy yielded $8.49 \pm 0.31\,g\,l^{-1}$ of isobutanol and $2.38 \pm 0.06\,g\,l^{-1}$ of 2-MBOH, with post-induction average yields of $53.5 \pm 8.4\,mg\,g^{-1}$ glucose for isobutanol (13% of theoretical maximum) and $14.17 \pm 2.57\,mg\,g^{-1}$ glucose of 2-MBOH, with measured instantaneous isobutanol yields of up to $270.6\,mg\,g^{-1}$ glucose (66% of theoretical yield) (Fig. 3e, Supplementary Table 5, Methods, Supplementary Results). Our mechanistic predictions of a darkness-induced metabolic shift to isobutanol biosynthesis are supported by quantitative PCR (qPCR) measurements of *PDC1* and *ILV2* mRNA levels (Extended Data Fig. 6b).

Optogenetics is a powerful way to control cellular physiology. Photosensitive proteins have had an enormous impact in neuroscience, cell biology and developmental biology by controlling ion channels, enzyme activity and gene expression[9,28–30]. Our work demonstrates that optogenetics also holds promise in metabolic engineering, enabling the reversible control and fine-tuning of engineered metabolic pathways.

Nevertheless, combining optogenetics and metabolic engineering has its challenges. The high cell densities usually associated with microbial fermentations might be predicted to severely limit light penetration, which is one reason we initially adopted our design of a darkness-induced production phase. However, additional experiments showed robust light-stimulated gene expression could be achieved even at cell densities as high as $OD_{600} = 50$ in 5-l bioreactors (Extended Data Fig. 10), suggesting that the high light sensitivity and strong levels of gene expression achieved by the current generation of optogenetic tools may be sufficient even in these challenging conditions. Even more potent responses to dim light could potentially be achieved by using well-characterized light-oxygen-voltage-sensing-domain (LOV) mutants with longer lit-state lifetimes[18] (our current VP16–EL222 remains in the photoactivated state for approximately 30 s; ref. 12), or other photoactive proteins with highly stable light-switchable conformations[13] (see Supplementary Discussion). For fermentation conditions that pose a greater challenge to light penetration than in this study, our OptoINVRT circuits offer a solution to control gene expression as they do not require light during the fermentation.

We used optogenetic regulation of engineered metabolic pathways to address the long-standing challenge of ethanol competition in branched-chain alcohol production. We and others have developed triple PDC deletion strains (*PDC1*Δ, *PDC5*Δ, *PDC6*Δ) that recovered their ability to grow on glucose by directed evolution[23]. However, efforts to produce isobutanol in these strains from mitochondrial (unpublished results) or cytosolic[31] biosynthetic pathways have thus far been unsuccessful. Our light-controlled metabolic valve offers an effective alternative to genetically deleting essential pathways that compete with a pathway of interest[5]. This allowed us to surpass the highest titres of isobutanol and 2-MBOH reported for yeast in the peer-reviewed literature that we have analysed by fivefold (Supplementary Table 6) and 20-fold[25], respectively, making a strong case for the application of optogenetics to metabolic engineering.

Optogenetic regulation of metabolic pathways enables new strategies for optimizing engineered pathways and fermentation conditions using periodic light pulses. Although further development for industrial applications is needed, in the future, light inputs delivered to a bioreactor could be automatically controlled in response to feedback from different fermentation outputs (for example, optical density or the readout of biosensors), providing unprecedented capabilities for operating, optimizing and automating fermentations for valuable product biosynthesis.

Online Content Methods, along with any additional Extended Data display items and Source Data, are available in the online version of the paper; references unique to these sections appear only in the online paper.

Received 4 May 2017; accepted 13 February 2018.
Published online 21 March 2018.

1. Woolston, B. M., Edgar, S. & Stephanopoulos, G. Metabolic engineering: past and future. *Annu. Rev. Chem. Biomol. Eng.* **4,** 259–288 (2013).
2. Zhang, Y. *et al.* Using unnatural protein fusions to engineer resveratrol biosynthesis in yeast and Mammalian cells. *J. Am. Chem. Soc.* **128,** 13030–13031 (2006).
3. Keasling, J. D. Manufacturing molecules through metabolic engineering. *Science* **330,** 1355–1358 (2010).
4. Ajikumar, P. K. *et al.* Isoprenoid pathway optimization for Taxol precursor overproduction in *Escherichia coli*. *Science* **330,** 70–74 (2010).
5. Tan, S. Z., Manchester, S. & Prather, K. L. J. Controlling central carbon metabolism for improved pathway yields in *Saccharomyces cerevisiae*. *ACS Synth. Biol.* **5,** 116–124 (2015).
6. Ro, D. K. *et al.* Production of the antimalarial drug precursor artemisinic acid in engineered yeast. *Nature* **440,** 940–943 (2006).
7. Gu, P., Su, T., Wang, Q., Liang, Q. & Qi, Q. Tunable switch mediated shikimate biosynthesis in an engineered non-auxotrophic *Escherichia coli*. *Sci. Rep.* **6,** 29745 (2016).

8. Brockman, I. M. & Prather, K. L. J. Dynamic knockdown of *E. coli* central metabolism for redirecting fluxes of primary metabolites. *Metab. Eng.* **28,** 104–113 (2015).
9. Toettcher, J. E., Voigt, C. A., Weiner, O. D. & Lim, W. A. The promise of optogenetics in cell biology: interrogating molecular circuits in space and time. *Nat. Methods* **8,** 35–38 (2011).
10. Milias-Argeitis, A. *et al. In silico* feedback for *in vivo* regulation of a gene expression circuit. *Nat. Biotechnol.* **29,** 1114–1116 (2011).
11. Kennedy, M. J. *et al.* Rapid blue-light-mediated induction of protein interactions in living cells. *Nat. Methods* **7,** 973–975 (2010).
12. Motta-Mena, L. B. *et al.* An optogenetic gene expression system with rapid activation and deactivation kinetics. *Nat. Chem. Biol.* **10,** 196–202 (2014).
13. Shimizu-Sato, S., Huq, E., Tepperman, J. M. & Quail, P. H. A light-switchable gene promoter system. *Nat. Biotechnol.* **20,** 1041–1044 (2002).
14. Taslimi, A. *et al.* Optimized second-generation CRY2-CIB dimerizers and photoactivatable Cre recombinase. *Nat. Chem. Biol.* **12,** 425–430 (2016).
15. Salinas, F., Rojas, V., Delgado, V., Agosin, E. & Larrondo, L. F. Optogenetic switches for light-controlled gene expression in yeast. *Appl. Microbiol. Biotechnol.* **101,** 2629–2640 (2017).
16. Nash, A. I. *et al.* Structural basis of photosensitivity in a bacterial light-oxygen-voltage/helix-turn-helix (LOV-HTH) DNA-binding protein. *Proc. Natl Acad. Sci. USA* **108,** 9449–9454 (2012).
17. Rivera-Cancel, G., Motta-Mena, L. B. & Gardner, K. H. Identification of natural and artificial DNA substrates for light-activated LOV-HTH transcription factor EL222. *Biochemistry* **51,** 10024–10034 (2012).
18. Zoltowski, B. D., Motta-Mena, L. B. & Gardner, K. H. Blue light-induced dimerization of a bacterial LOV-HTH DNA-binding protein. *Biochemistry* **52,** 6653–6661 (2013).
19. Reade, A. *et al.* TAEL: a zebrafish-optimized optogenetic gene expression system with fine spatial and temporal control. *Development* **144,** 345–355 (2017).
20. Jayaraman, P. *et al.* Blue light-mediated transcriptional activation and repression of gene expression in bacteria. *Nucleic Acids Res.* **44,** 6994–7005 (2016).
21. Da Silva, N. A. & Srikrishnan, S. Introduction and expression of genes for metabolic engineering applications in *Saccharomyces cerevisiae*. *FEMS Yeast Res.* **12,** 197–214 (2012).
22. Usherenko, S. *et al.* Photo-sensitive degron variants for tuning protein stability by light. *BMC Syst. Biol.* **8,** 128 (2014).
23. van Maris, A. J. A. *et al.* Directed evolution of pyruvate decarboxylase-negative *Saccharomyces cerevisiae*, yielding a C_2-independent, glucose-tolerant, and pyruvate-hyperproducing yeast. *Appl. Environ. Microbiol.* **70,** 159–166 (2004).
24. Klein, J. L. C., Olsson, L. & Nielsen, J. Glucose control in *Saccharomyces cerevisiae* : the role of *MIG1* in metabolic functions. *Microbiology* **144,** 13–24 (1998).
25. Avalos, J. L., Fink, G. R. & Stephanopoulos, G. Compartmentalization of metabolic pathways in yeast mitochondria improves the production of branched-chain alcohols. *Nat. Biotechnol.* **31,** 335–341 (2013).
26. Hammer, S. K. & Avalos, J. L. Uncovering the role of branched-chain amino acid transaminases in *Saccharomyces cerevisiae* isobutanol biosynthesis. *Metab. Eng.* **44,** 302–312 (2017).
27. Park, S. H., Kim, S. & Hahn, J. S. Improvement of isobutanol production in *Saccharomyces cerevisiae* by increasing mitochondrial import of pyruvate through mitochondrial pyruvate carrier. *Appl. Microbiol. Biotechnol.* **100,** 7591–7598 (2016).
28. Deisseroth, K. Optogenetics. *Nat. Methods* **8,** 26–29 (2011).
29. Gerhardt, K. P. *et al.* An open-hardware platform for optogenetics and photobiology. *Sci. Rep.* **6,** 35363 (2016).
30. Milias-Argeitis, A., Rullan, M., Aoki, S. K., Buchmann, P. & Khammash, M. Automated optogenetic feedback control for precise and robust regulation of gene expression and cell growth. *Nat. Commun.* **7,** 12546 (2016).
31. Milne, N., Wahl, S. A., van Maris, A. J. A., Pronk, J. T. & Daran, J. M. Excessive by-product formation: a key contributor to low isobutanol yields of engineered *Saccharomyces cerevisiae* strains. *Metab. Eng. Commun.* **3,** 39–51 (2016).

Supplementary Information is available in the online version of the paper.

Acknowledgements We thank K. Gardner and L. Motta-Mena for providing the plasmids and maps for the EL222 system (pVP16–EL222 and pC120-Fluc)[12], D. Pincus for plasmid pNH603, J. J. Lee for plasmid pET28a Ldh, C. Taxis for plasmid pDS143, C. Nelson for sharing her qPCR equipment, S. Han for assistance in qPCR experiments and figure presentation, J. Rabinowitz and J. Storey for sharing their 500-ml Sixfors fermentation system for fed-batch fermentation experiments, S. Silverman for technical assistance on this equipment and C. DeCoste and the Princeton Molecular Biology Flow Cytometry Resource Center for assistance in flow cytometry experiments. This work was supported by the Alfred P. Sloan Foundation (to J.L.A.), The Pew Charitable Trusts (to J.L.A.), National Institutes of Health grant DP2EB024247 (to J.E.T.) and an Eric and Wendy Schmidt Transformative Technology Fund grant (to J.L.A. and J.E.T.).

Author Contributions E.M.Z., J.E.T. and J.L.A. conceived this project and designed the experiments. E.M.Z., Y.Z. and J.L.A. constructed the strains and plasmids. E.M.Z. and H.P. performed the experiments that are shown in Fig. 1; E.M.Z. and J.M. conducted experiments illustrated in Fig. 2; E.M.Z. performed experiments that are shown in Fig. 3; E.M.Z. performed experiments illustrated in Extended Data Figs 1–10. Y.Z. performed experiments illustrated in Extended Data Figs 1, 8. M.A.L. performed experiments illustrated in Extended Data Fig. 10. E.M.Z., J.E.T. and J.L.A. analysed the data and wrote the paper.

Author Information Reprints and permissions information is available at www.nature.com/reprints. The authors declare no competing interests. Readers are welcome to comment on the online version of the paper. Publisher's note: Springer Nature remains neutral with regard to jurisdictional claims in published maps and institutional affiliations. Correspondence and requests for materials should be addressed to J.L.A. (javalos@princeton.edu) or J.E.T. (toettcher@princeton.edu).

Reviewer Information *Nature* thanks L. Larrondo and the other anonymous reviewer(s) for their contribution to the peer review of this work.

METHODS

Assembly of DNA constructs. We cloned promoter-gene-terminator sequences into previously described standardized vector series (pJLA vectors)[25]. This allows for easy manipulation and generation of multi-gene plasmids. All genes were designed to have NheI and XhoI restriction sites at the 5′ and 3′ ends, respectively, which were used to insert the genes into pJLA vectors. Each promoter-gene-terminator construct is flanked by XmaI and AgeI restriction sites at their 5′ ends, and MreI, AscI and BspEI sites at their 3′ ends, which we used for easy assembly of multi-gene plasmids, as previously described[25] (Supplementary Table 1).

Qiagen Miniprep, Qiagen Gel Extraction and Qiagen PCR purification kits were used to extract and purify plasmids and DNA fragments. Most genes and promoters (*ILV2*, *ILV3*, *ILV5*, *ARO10*, LlAdhA^{RE1} (ref. 32), *GAL4*, *GAL80*, GFP, P_{GAL1}, P_{TEF}, P_{TDH3}, P_{PGK1}, P_{CYC1}, P_{ADH1}) were amplified from yeast genomic DNA or laboratory plasmids, using Phusion polymerase from NEB, according to the manufacturer's instructions. Other genes were amplified from plasmids provided by other groups: PsLdh from plasmid pET28a, Ldh[33,34] from J. J. Lee; and the photosensitive degron derived from the fusion of the LOV2–V19L domain of phototropin 1 from *Arabidopsis thaliana* and a synthetic degradation sequence derived from the murine (mouse) ornithine decarboxylase from plasmid pDS143 from C. Taxis[22]. The codon-optimized sequence for VP16–EL222 was purchased as a gBlock from IDT. The sequence for the P_{C120} promoter was synthesized by the Bio Basic gene synthesis service. When pJLA vectors were not available, we used Gibson isothermal assembly to produce our constructs, based on published protocols[35]. Enzymes were purchased from NEB (XmaI, AscI, NheI, XhoI, BspEI, AgeI, T4 DNA ligase, Phusion Polymerase) and Thermo Fisher Scientific (MreI).

We modified the single copy integration plasmid pNH603[36] to make a plasmid compatible with the pJLA vectors that can be used to introduce gene cassettes into the *HIS3* locus. We first removed the AscI site of pNH603 and replaced the *ADH1* terminator (T_{ADH1}) sequence between PtsI and SacI with a fragment containing an XmaI restriction site. Then we introduced a cloning sequence array consisting of XmaI, MreI, AscI and BspEI between the XmaI site (which replaced the T_{ADH1}) and KpnI restrictions sites, to make pYZ12-B (Extended Data Fig. 1a, Supplementary Table 1). This addition makes pYZ12-B compatible with the pJLA platform of vectors, and allowed for easy transfer of gene cassettes from pJLA 2μ plasmids. Gene constructs in pYZ12-B were integrated into the *HIS3* locus of the genome by linearizing the plasmid with PmeI. We also used pRSII416[37] to introduce genes in a single copy episomal plasmid (CEN); this was done by inserting promoter–gene–terminator constructs cut from pJLA vectors with XmaI and MreI and inserting at the XmaI site of pRSII416.

Similar to pYZ12-B, we developed pYZ23 (Supplementary Table 1, Extended Data Fig. 1b), a pJLA vector-compatible plasmid, to integrate multiple copies of gene constructs into the δ-sites of the yeast genome. The pYZ23 plasmid targets the YARCdelta5, the 337-bp-long terminal repeat (LTR) of *S. cerevisiae* Ty1 retrotransposons (YARCTy1-1, SGD ID: S000006792)[38]. We constructed pYZ23 with four overlapping DNA fragments using the Gibson isothermal assembly method[35]. The four fragments are: (1) the PmeI-linearized backbone fragment from pYZ12-B containing the ampicillin-resistance gene; (2) the first 207 bp of the YARCdelta5 LTR; and (3) the last 218 bp of the YARCdelta5 LTR, both of which were amplified from the BY4741 genome using primer pairs Yfz_Oli39 and Yfz_Oli40, and Yfz_Oli43 and Yfz_Oli44, respectively (Supplementary Table 7); and (4) the BleMX6 gene cassette from pCY 3090-07 (Addgene 36232), amplified using primers Yfz_Oli41 and Yfz_Oli42 (Supplementary Table 7), which add flanking *loxP* sites (*lox66* and *lox71*) to the *BleMX6* gene. Additional restriction sites, including MreI, AscI and BspEI, were introduced for subcloning (Extended Data Fig. 1b, Supplementary Table 7).

All vectors were sequenced using Sanger sequencing from GENEWIZ before using them to transform yeast. We avoid using tandem repeats to prevent recombination after yeast transformation (Extended Data Fig. 1c), and thus do not observe instability of plasmids.

Yeast transformations. Yeast transformations were carried out using standard lithium acetate protocols, and the resulting strains are catalogued in Supplementary Table 2. Gene constructs derived from pYZ12-B and pYZ23 vectors were genomically integrated into the *HIS3* locus and δ-sites (YARCdelta5), respectively. These vectors were first linearized with PmeI and DNA fragments were purified using a Qiagen PCR purification kit before using them for yeast transformation. Gene deletions were carried out using homologous recombination strategies. DNA fragments containing antibiotic resistance cassettes flanked with *loxP* sites were amplified using PCR from pAG26[39] (containing the hygromycin resistance gene, hygromycin B phosphotransferase (*HygB*-PT)), pUG6[40] (containing the G418 resistance gene *KanMX*), or pAG36[39] (containing the nourseothricin resistance gene *NAT1*), using primers with 40 bp of homology to the promoter and terminator regions of the gene targeted for deletion. Antibiotic-resistance markers were subsequently removed by expressing Cre recombinase from the pSH62 (AF298785) vector[41]. After transformation, cells were plated on synthetic complete (SC) drop out medium depending on the auxotrophy restored by the construct. In the case of antibiotic selection, cells were plated onto non-selective YPD plates for 16 h, then replica plated onto YPD plates with 300 μg ml^{-1} hygromycin (purchased from Invitrogen), 200 μg ml^{-1} nourseothricin (purchased from WERNER BioAgents), or 200 μg ml^{-1} G418, purchased from Gibco by Life Technologies). Zeocin was used to select for δ-integration at concentrations ranging from 800 to 1,200 μg ml^{-1} (purchased from Thermo Fisher Scientific).

All strains with genomic integrations or gene deletions were genotyped with PCR to confirm their accuracy. We integrated constructs in the *HIS3* locus or δ-sites to promote strain stability.

Yeast cell culture growth, centrifugation and optical measurements. Unless otherwise specified, liquid yeast cultures were grown in 24-well plates, at 30 °C and shaken at 200 r.p.m., in either YPD or SC-dropout medium supplemented with 2% glucose. SC-dropout media include 94.8 mg l^{-1} of valine, 94.8 mg l^{-1} of isoleucine and 189.6 mg l^{-1} of leucine along with all other necessary standard nutrients unless otherwise specified. To stimulate cells with light, we used blue light-emitting diode (LED) panels (HQRP New Square 12-inch Grow Light Blue LED 14W), placed 40 cm from cell cultures. To control light duty cycles, the LED panels were regulated with a Nearpow Multifunctional Infinite Loop Programmable Plug-in Digital Timer Switch (purchased from Amazon). To resuspend cells in new media, cell cultures were centrifuged in a table-top centrifuge, with 24-well plate rotor adaptors. Unless otherwise specified, plates were centrifuged at 234*g* for 5 min.

Fluorescence and OD_{600} measurements were taken using a TECAN plate reader (infinite M200PRO). The excitation and emission wavelengths used for GFP fluorescence measurements were 485 nm and 535 nm, respectively, using an optimal gain for all measurements. To process fluorescence data, the background fluorescence from the medium was first subtracted from values. Then, the GFP/OD_{600} values of cells lacking a GFP construct were subtracted from the fluorescence values (GFP/OD_{600}) of each sample to normalize for light bleaching of the medium and cell contents. Thus, reported values were calculated according to the following formula

$$\mathrm{GFP/OD}_{\mathrm{strain,condition}} = \frac{\mathrm{GFP}_{\mathrm{strain,condition}} - \mathrm{GFP}_{\mathrm{media,condition}}}{\mathrm{OD}_{\mathrm{strain,condition}} - \mathrm{OD}_{\mathrm{media,condition}}} - \frac{\mathrm{GFP}_{\mathrm{no\ GFP\ control\ strain,condition}} - \mathrm{GFP}_{\mathrm{media,condition}}}{\mathrm{OD}_{\mathrm{no\ GFP\ control\ strain,condition}} - \mathrm{OD}_{\mathrm{media,condition}}}$$

All fluorescence measurements were done at the end of experiments or on samples taken from experimental cultures, such that potential activation of VP16–EL222 by the light used to excite GFP did not affect our experiments or results.

To measure cell concentration, optical-density measurements were taken at 600 nm, using medium (exposed to the same conditions as the yeast) as a blank. Measurements were performed using the TECAN plate reader (infinite M200PRO) or Eppendorf spectrophotometer (BioSpectrometer basic), from samples diluted to a range of OD_{600} of 0.1 to 1.0.

All experiments involving light-inducible strains were done under minimal ambient light, unless otherwise specified, to avoid unwanted activation of optogenetic systems.

Construction of OptoEXP system. We purchased a gBlock (IDT) containing the yeast codon-optimized sequence of VP16–EL222, flanked by NheI and XhoI restriction sites, which we inserted into plasmid $pJLA121^{0301}$ (containing P_{PGK1} and T_{CYC1}). We then used XmaI and AscI to subclone P_{PGK1}–VP16–EL222–T_{CYC1} into pYZ12-B to make EZ-L105 (Supplementary Table 1), which allows single genomic integration of gene cassettes into the *HIS3* locus. We then changed the promoter to P_{TEF1} using XmaI and NheI restriction site cutting and subsequent ligation to make EZ-158, used for OptoEXP expression in glycerol media. In addition, we synthesized the C120 and minimal promoter sequence (TAGAGGGTATATAATGGAAGCTCGACTTCCAG), otherwise known as P_{C120}, using Bio Basic's gene synthesis service and used it to develop new pJLA vectors with the P_{C120} promoter and either an *ADH1* or *ACT1* terminator, making $pJLA121^{0803}$ or $pJLA121^{0802}$, respectively (Supplementary Table 1).

Characterization of OptoEXP. To test the OptoEXP system, we built plasmid EZ-L83 ($pJLA111\text{-}GFP^{0803}$), which places GFP under P_{C120} transcriptional control in a CEN/ARS plasmid with a *URA3* marker (Supplementary Table 1). We then used EZ-L105 to integrate a single copy of P_{PGK1}–VP16–EL222–T_{CYC1} construct into the *HIS3* locus of CENPK.2-1C, selecting strain YEZ24 from a SC lacking His (SC-His) plate supplemented with 2% glucose. Subsequently, we transformed YEZ24 with EZ-L83, and selected strain YEZ32 from a SC plate lacking uracil (SC-Ura) plate supplemented with 2% glucose. We also transformed YEZ24 with empty pRSII416 to make control strain YEZ32C, which has no GFP.

To characterize light induction by OptoEXP, we tested four different colonies of YEZ32. We grew cells from each colony in liquid SC-Ura overnight in the dark

(tin foiled). The next morning, we diluted the cells to OD_{600} of 0.1 in fresh SC-Ura, to a final volume of 1 ml each, incubated in individual wells of a 24-well clear Costar plate. We prepared five identical plates and tin foiled one of them. The plates were then placed in the dark (tin-foil-covered plate), under constant blue light, or under blue light with duty cycles of 5 s on and 75 s off, 8 s on and 72 s off and 11 s on and 69 s off, with a blue LED panel at 40 cm from each plate. We used duty cycles instead of light intensity to better control light dose and reproducibility (Extended Data Fig. 2). Cell cultures were grown for 8 h under blue light panels or in the dark, then their GFP fluorescence and OD_{600} were measured using the TECAN plate reader. Error bars represent the s.d. from biological replicates ($n = 4$).

To benchmark the combination of P_{PGK1}–VP16–EL222–T_{CYC1} and a single copy of P_{C120}, which we refer to as OptoEXP, we compared it to several constitutive promoters. To achieve this, we made pJLA111-GFP^{0X0X} constructs (CEN/ARS with *URA3* markers) containing P_{CYC1} (EZ-L64), P_{ADH1} (EZ-L63), P_{PGK1} (EZ-L67), P_{TDH3} (EZ-L65) and P_{TEF1} (EZ-L66), which we used to transform YEZ24 to make yeast stains YEZ27 (EZ-L64), YEZ28 (EZ-L63), YEZ29 (EZ-L67), YEZ30 (EZ-L65) and YEZ31 (EZ-L66).

YEZ32C was used as a control with no GFP production for strains with pJLA111-GFP^{0X0X} plasmids. YEZ27, YEZ28, YEZ29, YEZ30, YEZ31 and YEZ32 were tested similarly to the OptoEXP testing above (YEZ32).

Flow cytometry experiments. We used flow cytometry to determine whether the OptoEXP system produces a homogeneous response in the cell population. To construct strains for these experiments, we transformed CEN.PK2-1C with PmeI-linearized pYZ12-B (a non-fluorescent control), EZ-L136, EZ-L516 or EZ-L350 to make YEZ140 (CEN.PK2-1C with histidine prototrophy restored), YEZ139 (CEN.PK2-1C with OptoEXP driving GFP, and P_{PGK1} driving VP16–EL222, which works best in glucose), YEZ243 (CEN.PK2-1C with OptoEXP driving GFP, and P_{TEF1} driving VP16–EL222, which works well in glucose or glycerol) or YEZ186 (CEN.PK-2C with *HIS3*::P_{TEF1}–GFP–T_{ACT1}, for constitutive expression of GFP as control), respectively.

To test the homogeneity of gene expression of OptoEXP we grew overnight cultures of YEZ139, YEZ140 and YEZ186 in SC-His medium supplemented with 2% glucose in the dark. The next morning, we diluted 20 µl of these cultures into 980 µl of fresh medium in two 24-well plates. Both plates were placed in the dark and shaken at 200 r.p.m. at 30 °C for 3 h. Then, one plate was placed 40 cm below a blue light panel and the other was tin foiled and kept in the dark. Both plates were shaken at 200 r.p.m. at 30 °C for 3 h. Then, 5 µl of culture was diluted into 995 µl of PBS and used for flow cytometry (Extended Data Fig. 2a, b). Samples were run in triplicates from three different cultures separated after the overnight stage. Representative samples from these triplicates were chosen for the figures.

To test OptoEXP performance in non-fermentative conditions, we grew 10-ml overnight cultures of YEZ243, YEZ140 and YEZ186 in SC-His medium supplemented with 3% glycerol and 2% ethanol, in tin-foiled tubes (in the dark) in the roller drum. The next morning, we diluted 30 µl of these cultures into 980 µl of fresh medium to an OD_{600} of 0.05–0.1 in four 24-well plates. All four plates were placed in the dark (tin foiled) and shaken at 200 r.p.m. at 30 °C for 6 h (until the yeasts were in the exponential growth phase, OD_{600} of approximately 3). Then, one plate was placed 40 cm below a blue light panel and the others were kept tin foiled (in the dark). After 1 h, another plate was moved into the light. After another half hour more, another plate was moved into the light. All plates were kept shaken at 200 r.p.m. at 30 °C for 2 h after the initial 6 h of growth. Then, 5 µl of each culture was diluted into 995 µl of PBS medium and used for flow cytometry (Extended Data Fig. 2c). Samples were run in triplicates from three different cultures separated after the overnight stage. Representative samples from these triplicates were chosen for the figures.

GFP expression was quantified by flow cytometry using a BD LSR II flow cytometer (BD Biosciences) with an excitation wavelength of 488 nm and an emission wavelength of 530 nm. The gating used in our analyses was defined to include positive (YEZ186) and negative (YEZ140) control cells based on GFP fluorescence, but exclude particles that are either too small or too large to be single living yeast cells, based on the side scatter (SSC-A) versus forward scatter (FSC-A) plots (Extended Data Fig. 2d). Mean fluorescence values were determined from 20,000 cells. Data were analysed with the FlowJo v.10 software (Tree Star).

All fluorescence measurements were performed at the end of experiments or on samples taken from experimental cultures, such that potential activation of VP16–EL222 by the light used to excite GFP did not affect our experiments or results.

Construction of the OptoINVRT circuits. OptoINVRT circuits were initially developed and characterized in two yeast strain backgrounds: YEZ44 (CENPK.2-1C, *GAL80*Δ, *GAL4*Δ) and Y202 (S288C, *PDC1*Δ, *PDC5*Δ, *PDC6*Δ, *GAL80*Δ, containing pJLA121-PDC1^{0202}), (Supplementary Table 2).

Gene circuits were assembled using restriction enzyme digests and ligations afforded by pJLA vectors, in which open reading frames were inserted using NheI and XhoI sites, and multiple cassettes assembled using XmaI (or AgeI), MreI (or BspEI) and AscI[25]. Each gene circuit was constructed by assembling five promoter–gene–terminator sequences into single integration vectors targeting the *HIS3* locus (EZ-L259, EZ-L260 and EZ-L266; Supplementary Tables 1, 3). The PSD used in OptoINVRT3 is derived from the fusion of phototropin1 LOV2 domain (V19L mutant) from *A. thaliana* and a synthetic degradation sequence derived from the murine ornithine decarboxylase[22]. This PSD was fused to the C terminus of *GAL4* using Gibson assembly of pJLA121^{0303} cut with XhoI and PSD amplified from pDS143[22] with overhang sequences of 30 bp that are homologous to the multiple cloning sequence and T_{ADH1} of pJLA121^{0303} to make EZ-L247, to which we then inserted *GAL4* using NheI and XhoI through ligation to make the precursor plasmid of EZ-L266 (EZ-L251).

Characterization of OptoINVRT circuits. The three OptoINVRT circuits, controlling GFP expression, were initially characterized by transforming YEZ44 to produce YEZ100 (OptoINVRT1), YEZ101 (OptoINVRT2) and YEZ102 (OptoINVRT3), and Y202 to produce YEZ115 (OptoINVRT1), YEZ116 (OptoINVRT2) and YEZ117 (OptoINVRT3) (Supplementary Table 2). OptoINVRT circuits were characterized using strains YEZ100-102 and YEZ115-117 by performing the same experiment done on YEZ32, described above, to characterize the OptoEXP system. In this case, we exposed cells to full light, complete darkness, or light pulses of 8 s on and 72 s off. YEZ186 and YEZ140 were used as controls for strains derived from YEZ44, and YEZ171 and YEZ94 were used as controls for strains derived from Y202.

Characterization of light panels. The light intensity of panels was measured using a Quantum meter with a separate sensor (Model MQ-510 from Apogee Instruments), placed 40 cm from the light panel of interest (the same distance was used for all 24-well plate experiments). The resulting intensities ranged from 53 to 134 µmol $m^{-2} s^{-1}$ with an average of 77.5 µmol $m^{-2} s^{-1}$ (with 465 nm max peak spectra). Ambient light under these conditions ranged from 4–5 µmol $m^{-2} s^{-1}$. We then measured the levels of GFP expression in strains YEZ243 and YEZ186 (as well as YEZ140, as a negative control) induced by three different panels with 53, 82 or 134 µmol $m^{-2} s^{-1}$ intensities, placed 40 cm from the 24-well plates, using the same protocol for experiments shown in Fig. 1b. Overnight cultures grown in the dark where diluted to an OD_{600} of 0.1, and incubated for 8 h in either full light, or light pulses of 10 s on and 70 s off. The levels of GFP expression were indistinguishable across the three panels tested (including the brightest and dimmest panels used in this study), and responded uniformly to changes in light duty cycle (Extended Data Fig. 3). This demonstrates that there is no detectable difference between variations in the intensities of panels used in this study and that varying duty cycle is an effective way to control gene expression using our optogenetic transcriptional controls.

Development of an OptoEXP-PDC strain. Strain Y200 contains a triple gene deletion of *PDC1*Δ, *PDC5*Δ and *PDC6*Δ, as well as a 2µ-*URA3* plasmid pJLA121-PDC1^{0202} with P_{TEF1}–*PDC1*–T_{ACT1}, which allows it to grow robustly in glucose. Y200 was transformed with a PmeI-linearized EZ-L165 plasmid to insert a cassette composed of P_{TEF1}–VP16–EL222 –T_{CYC1} and P_{C120}–*PDC1*–T_{ADH1} into its *HIS3* locus, resulting in strain YEZ50 (Supplementary Tables 1, 2). As a control, we also transformed Y200 with PmeI-linearized EZ-L158, a vector containing P_{TEF1}–VP16–EL222–T_{CYC1} but lacking P_{C120}–PDC1–T_{ADH1}, and then counter-selected against the pJLA121-PDC1^{0202} plasmid by growing on 5-fluorootic acid (5-FOA) (as described below) to produce the control strain YEZ50C. Strain YEZ50 was then transformed with PmeI-linearized EZ-L143, which inserts multiple copies of P_{C120}–*PDC1*–T_{ADH1} into δ-integration sites of the yeast genome. Colonies able to grow on YPD plates containing 800 µg ml^{-1} of zeocin were replica plated on plates containing SC–His with 3% glycerol and 2% ethanol twice. The resulting plates were then replica plated on SC–His with 3% glycerol, 2% ethanol and 1 mg ml^{-1} 5-FOA, and then finally back onto plates containing SC-His with 3% glycerol and 2% ethanol. This treatment efficiently counter-selects against pJLA121-PDC1^{0202}, due to its *URA3* marker[42]. From this plate, we isolated YEZ61-23, a strain that can grow on SC-His with 2% glucose plates only when exposed to blue light, which is consistent with having *PDC1* expression controlled by P_{C120}, and VP16–EL222. As a control, we also transformed Y200 with PmeI-linearized EZ-L143, which contains P_{C120}–*PDC1*–T_{ADH1} but lacks P_{TEF1}–VP16–EL222–T_{CYC1}, and counter-selected against in pJLA121-PDC1^{0202} in 5-FOA to produce YEZ61C. This control strain has multiple copies of P_{C120}–*PDC*1–T_{ADH1} in δ-sites, but lacks the VP16–EL222 needed to transcribe them.

Light-dependent growth of an OptoEXP-PDC strain. *Solid media*. Cells from strains BY4741, YEZ61-23, YEZ50C and YEZ61C were patched onto an agar plate containing yeast extract, peptone and 3% glycerol and 2% ethanol (YPGE plate), and grown over night in ambient light. This plate was then replica plated onto a fresh YPGE plate and two YPD plates. One of the YPD plates was covered in tin foil and the other exposed to constant blue light, while the YPGE was left at ambient lighting. Replica plating was performed such that the YPD plate ultimately covered in tin foil was replicated first, the YPD plate ultimately exposed to constant blue

light was replicated second, and the YPGE plate was replicated last. All plates were incubated at 30 °C for 48 h (Fig. 2b).

Liquid media. Single colonies of YEZ61-23 and BY4741 were used to inoculate liquid SC-His with 2% glucose medium. The cells were grown for 24 h on a roller drum at 200 r.p.m., 30 °C and 40 cm away from a blue light source (HQRP New Square 12-inch LED Grow Light System 225 Blue LED 14W). Subsequently, the OD_{600} was measured with a spectrophotometer, and the cells were diluted to an OD_{600} of 0.1 in fresh SC-His medium supplemented with 2% glucose medium in three 1-ml replicates in four 24-well plates (Celltreat non-treated sterile flat bottom plates). Each plate was centred 40 cm under an HQRP blue light panel. One plate was exposed to full blue light. The other three plates were exposed to 10 s on and 70 s off of blue light, 20 s on and 60 s off of blue light or 40 s on and 40 s off of blue light. A fifth plate was wrapped in aluminium foil to incubate cells in the absence of light. OD readings were taken using a TECAN plate reader at 0 h, 10 h, 12.5 h, 13.5 h, 15 h, 17 h, 19 h, 20.5 h and 31.75 h. Readings were taken under minimal light conditions to prevent unwanted activation of EL222. Data are available in a supplementary spreadsheet.

The exponential growth phase of YEZ61-23 (identified as the most linear portion of the plot of $\log_e(OD)$ against time), was used to find the specific growth rates at different light doses. This was done by fitting the data to $\log_e(OD) = \log_e(OD_0) + \mu \times t$, using least squares linear regression, where OD_0 is a constant corresponding to the initial OD, and μ corresponds to the specific growth rate constant. The μ constants were calculated for each independent experiment and then averaged, with error bars representing s.d. ($n = 3$). Source Data are available with the online version of this paper.

Development of chemical production strains. To develop light-dependent lactic acid-producing strains, we transformed Y202 with PmeI-linearized EZ-L259, EZ-L260 and EZ-L266 (OptoINVRT1, OptoINVRT2 and OptoINVRT3 respectively) yielding YEZ115, YEZ116 and YEZ117. We then integrated multiple copies of PmeI-linearized EZ-L235 (Supplementary Table 1), which contains P_{C120} driving *PDC1* and P_{GAL1} driving the Ldh from *Pelodiscus sinensis* (provided by J. Lee) into δ-sites. Then we counter-selected against pJLA121-PDC1^{0202} to produce YEZ144 (OptoINVRT1), YEZ145 (OptoINVRT2) and YEZ146 (OptoINVRT3) (Supplementary Table 2). These strains induce *PDC1* and repress Ldh expression in the light; while in the dark they stop inducing *PDC1* and induce Ldh instead.

To develop light-dependent isobutanol-producing strains, we transformed YEZ115, YEZ116 and YEZ117 with PmeI-linearized EZ-L316, which integrates multiple copies of P_{C120}-driven *PDC1* and P_{GAL1}-driven *ILV2* in genomic δ-integration sites. We then counter-selected the transformants against pJLA121-PDC1^{0202} with 5-FOA to produce strains YEZ131 (OptoINVRT1), YEZ149 (OptoINVRT2) and YEZ133 (OptoINVRT3), respectively. Subsequently, we transformed these strains with plasmid EZ-L310 (Supplementary Table 1), which contains five genes from the mitochondrial isobutanol biosynthetic pathway: *ILV2*, *ILV5*, *ILV3*, *COX4–ARO10* and *COX4*–LlAdhA^{RE1} (ref. 25). The last two genes in EZ-L310 are fused by their N termini to the mitochondrial localization signal of *COX4*, ensuring that all five genes are targeted to the mitochondria[25]. In addition, P_{GAL1} drives *ILV2* expression, which places this gene under the control of the OptoINVRT circuits. The resulting strains are YEZ159, YEZ156 and HPY6 for OptoINVRT1, OptoINVRT2 and OptoINVRT3, respectively (Supplementary Table 2).

Screens for lactic acid- and isobutanol-producing strains. Colonies from each transformation plate (grown in glucose and under blue light) were screened for lactic acid (7 colonies from each of YEZ144, YEZ145 and YEZ146) or isobutanol (12 colonies from each of YEZ159, YEZ156 and HPY6) production (Supplementary Table 2). Each colony was used to inoculate 1 ml SC-His medium supplemented with 2% glucose (for lactic acid-producing strains) or SC-Ura medium supplemented with 2% glucose (for isobutanol-producing strains) in 24-well plates and grown overnight at 30 °C, 200 r.p.m. and blue light. The next morning, each culture was diluted to an OD_{600} of 0.1 for lactic acid-producing strains, or an OD_{600} of 0.15 for isobutanol-producing strains, in fresh medium, and grown for 12 h (for lactic acid production) or 18 h (for isobutanol production), at 30 °C, 200 r.p.m. and under blue light. After these incubation periods, the cultures reached OD_{600} values of 5 (for lactic acid-producing strains, $\rho = 5$) and 5 and 8 (for isobutanol-producing strains, $\rho = 8$, $\rho = 5$); at which point they were moved into the dark for 6 h for lactic acid-producing strains ($\theta = 6$ h) and 3 h for isobutanol-producing strains ($\theta = 3$ h). The cultures were then centrifuged and re-suspended in fresh medium, in plates that were then sealed with Nunc Sealing Tape (Thermo Fisher Scientific) to begin the fermentations. The plates were incubated in the dark at 30 °C and shaken at 200 r.p.m. for 48 h during fermentation. Subsequently, the cultures were centrifuged, and the supernatants collected for high-performance liquid chromatography (HPLC) analysis. For lactic acid-producing strains, most of the seven colonies screened for each OptoINVRT circuit produced similar amounts of lactic acid, with colonies of strain YEZ145 (containing OptoINVRT2) producing the highest titres (Extended Data Fig. 4c). On the other hand, out of the 12 colonies screened for each isobutanol-producing strain, only 2 or 3 produced high titres for each OptoINVRT circuit, with YEZ159 (containing OptoINVRT1) producing the highest titres (Extended Data Fig. 4d, e).

Construction of a high isobutanol-producing strain. We deleted *BAT1* from YEZ131 via homologous recombination, using the HygB hygromycin-resistance marker, resulting in strain YEZ158. Subsequently, we transformed YEZ158 with EZ-L310, resulting in transformants YEZ167, from which we screened 7 colonies, as described above, and identified YEZ167-4 as the strain with highest isobutanol production.

Optimizing experimental parameters for light-dependent fermentation. The colonies producing the highest titres from YEZ144, YEZ145 and YEZ146 (for lactic acid) and of YEZ167 (specifically YEZ167-4 for isobutanol), were used to optimize the pre-growth parameters of fermentation for lactic acid or isobutanol production. For each strain, an overnight culture was grown in blue light at 30 °C with shaking at 200 r.p.m., in SC medium supplemented with 2% glucose (SC-His for lactic acid-producing strains and SC-Ura for isobutanol-producing strains). To find the optimal cell density at which to switch cultures from light to dark, we diluted the overnight cultures into 1 ml SC-dropout medium to different OD_{600} values, ranging from 0.04 to 0.32. The lactic acid-producing strains were then grown for 16 h under 15 s on and 65 s off blue light cycles. The isobutanol-producing strains were grown for 18 h under 15 s on and 65 s off blue light cycles. We then measured the OD_{600} of each culture (these values correspond to variations in ρ), and incubated them in the dark for 6 h for lactic acid-producing strains ($\theta = 6$ h) and 3 h for isobutanol-producing strains ($\theta = 3$ h). After this dark incubation period, the cultures were centrifuged at 234*g* for 5 min and suspended in fresh SC-dropout medium containing glucose at 26.5 g l^{-1} (for lactic-acid-producing strains) or 21.5 g l^{-1} (for isobutanol-producing strains). The plates were sealed with Nunc Sealing Tape, and incubated in the dark for fermentation at 30 °C and 200 r.p.m. Control cultures were grown under 15 s on and 65 s off blue light during the growth phase, the dark incubation period, and the fermentation. Cultures producing lactic acid were harvested after 48 h, while samples of cultures producing isobutanol were taken after 24, 48 and 72 h. Cultures were centrifuged at 234*g* for 10 min, and supernatants were analysed with HPLC.

To optimize the dark incubation period immediately before fermentation (θ), the best isobutanol-producing strain, YEZ167-4, was grown overnight under 15 s on 65 s off blue light in SC-Ura medium supplemented with 2% glucose. The overnight culture was then diluted into seven different plates in quadruplicate samples in fresh medium to a starting OD_{600} of 0.1. The cultures were then grown to an OD_{600} of 8.5 (which was found to be the optimal OD_{600} in our previous experiment). At that point, the plates were tin foiled to ensure complete darkness. After every hour, one of the plates was centrifuged, and the cells suspended in fresh SC-Ura medium with 20.8 g l^{-1} glucose medium and subjected to a 48-h fermentation in the dark.

Optimizing the frequency of light bouts during the production phase of batch fermentation. A single colony of the best isobutanol-producing strain, YEZ167-4, was used to inoculate 5 ml SC-Ura medium supplemented with 4% glucose and grown overnight under light. The next morning, the culture was diluted in 1 ml fresh medium to an OD_{600} of 0.2 (in quadruplicates) and grown under light for 20 h to an OD_{600} of 9.5. Subsequently, the cultures were incubated for 3 h in the dark. To start the fermentations, the cultures were centrifuged again, and suspended in fresh SC-Ura medium supplemented with 15% glucose (precisely 157.0 g^{-1} glucose, as measured with HPLC), and kept in the dark. During the fermentation, the cultures were first exposed to 4 h of light and then pulsed every 5, 10, or 20 h for 30 min, at a duty cycle of 15 s on and 65 s off. As controls, some plates were always kept in the dark or in full light. Fermentations lasted for 80 h, after which the cultures were centrifuged, and the supernatants were analysed with HPLC.

NAD^+/NADH ratio measurements. YEZ167-4 was inoculated into 3 ml SC-Ura medium supplemented with 2% glucose and grown overnight under light at 30 °C and 200 r.p.m. The next morning, the culture was diluted into 1 ml fresh medium in 6 different 24-well plates to an OD_{600} of 0.2 (in quadruplicates) and grown at 30 °C and shaken at 200 r.p.m. under light for 20 h to an OD_{600} of 9.5. Subsequently, the cultures were incubated under the same conditions for 3 h in the dark. The cultures were then centrifuged at 234*g* for 5 min and resuspended in fresh SC-Ura medium supplemented with 15% glucose (precisely 157.0 g l^{-1} glucose, as measured with HPLC), and kept in the dark. As controls, one plate was always kept in the dark and one plate was kept in full light. The remaining four plates were pulsed every 10 h for 30 min, at a duty cycle of 15 s on and 65 s off. One plate was exposed to an extra 30-min pulse of light at a duty cycle of 15 s on and 65 s off precisely 4 h before harvest and placed back into the dark for the remainder of the fermentation. One plate was exposed to an extra 30-min pulse of light at a duty cycle of 15 s on and 65 s off precisely 2 h before harvest and placed back into the dark for the remainder of the fermentation. One plate was exposed to an extra 30-min pulse of light at

a duty cycle of 15 s on and 65 s off precisely 30 min before harvesting to test how the light pulses affect the NAD^+/NADH ratio. After 48 h, cells were harvested by centrifuging at 9,000*g* for 5 min and removing all supernatant. The NAD^+/NADH ratios of the pelleted cells were measured as previously described[43].

Light-dependent growth in a 2-l bioreactor. To test whether light penetration becomes limiting to a strain with light-dependent growth, we used a 2-l photobioreactor to compare the growth of YEZ167-4 (which is an isobutanol-producing strain with light-dependent growth) to that of YZy335 (which is a strain that constitutively produces isobutanol and is PDC^+, and thus its growth and isobutanol production are independent of light).

We used a single colony of YEZ167-4 or YZy335 to inoculate 5 ml SC-Ura medium supplemented with 2% glucose under light, overnight. The next morning, we diluted the culture in 0.5 l SC-Ura medium supplemented with 15% glucose to an OD_{600} of 0.1 in a UTEX 2-l glass photobioreactor surrounded by three blue light panels, placed 1 cm from its glass wall (Extended Data Fig. 9a, b), instead of the UTEX LED lighting platform. The culture was grown for 84 h at 30 °C and under constant blue illumination, with cells gently mixed with a magnetic stir bar and air sparging. Samples were taken every 12 h to measure the OD_{600} of the cell cultures (Fig. 3d). We report the average measurements of three independent fermentations for each strain, and the error bars correspond to the standard deviations of those three measurements.

Fed-batch fermentation. To test the capability of these systems to utilize higher amounts of glucose in a laboratory-scale fermenter, we conducted fed-batch experiments using the Sixfors INFORS AG CH-4103 Boltmingen/Switzerland based on a previously described protocol[44]. We did not sparge air to keep the fermentation in microaerobic conditions. The pH was set to 5.5 and maintained with a 0.5 M KOH feed. We autoclaved the 500-ml fermenter with 250 ml ddH_2O and exchanged the ddH_2O (using the air pump) with filtered 250 ml SC-Ura medium supplemented with 10% glucose. We used a single colony of YEZ167-4 to inoculate 5 ml SC-Ura medium supplemented with 2% glucose under light, overnight. The next day, we added the inoculum to the fermenter to obtain an OD_{600} of 0.2. The fermentation was kept at 30 °C and mixed at 200 r.p.m. Two light panels were placed 0.5 cm away from the vessel walls (Extended Data Fig. 9c, d), and kept on for the first 46 h (growth phase of the fermentation), in which the culture grew to an OD_{600} of 8.2 ± 0.1. The culture was then covered with black cloth and the light was turned off for 4 h. We then started a glucose feed of SC-Ura medium supplemented with 50% glucose at a rate of 2.9 ml h^{-1} for 90 h (run 1) or 120 h (runs 2 and 3) and turned on the light (continuously) for the first 4 h of the glucose feed. After the initial 4 h, the light was switched to a duty cycle of 45 min on and 7 h 15 min off for the remainder of the fermentation (production phase). Samples of 1 ml were taken at hours 0, 24, 48, 72, 96, 120, 144, 168, 192, 216, 240, 264 (after inoculation), for both OD_{600} measurements, and HPLC analysis. Samples collected at 48, 96, 144, 192 and 264 h were also analysed with qPCR.

Analysis of chemical concentrations. The concentrations of glucose, lactic acid, ethanol, isobutanol and 2-methyl-1-butanol were quantified with HPLC, using an Agilent 1260 Infinity instrument (Agilent Technologies). Samples were centrifuged to remove cells and other solid debris at 234*g* for 10 min, and the supernatants were then centrifuged for 30 min at 17,000*g* and 4 °C prior to loading onto an Aminex HPX-87H ion-exchange column (Bio-Rad). The column was eluted with a mobile phase of 5 mM sulfuric acid at 55 °C and a flow rate of 0.6 ml min^{-1}. Glucose, lactic acid, ethanol, isobutanol, and 2-methyl-1-butanol were monitored with a refractive index detector (RID). To determine their concentration, the peak areas were measured and compared to those of standard solutions for quantification.

Quantification of gene expression and δ-integration copy number. To measure the number of copies of P_{C120}–*PDC1* integrated into the genome of YEZ50lost, YEZ61-23, YEZ144, YEZ145, YEZ146 and YEZ167-4, we ran qPCR experiments on their genomic DNA, extracted with phenol–chloroform[45]. As a control strain containing a single copy of *PDC1*, we developed YEZ50lost by counter-selecting against plasmid pJLA121-$PDC1^{0202}$ from strain YEZ50, using 5-FOA as described above.

To quantify the expression of *PDC1* and *ILV2* during the fed-batch fermentation experiments, we measured transcript levels using qPCR. We collected 5 ml samples over the course of the fermentation and centrifuged them at 900*g* for 1.5 min. The mRNA was then extracted with phenol–chloroform[45]. Concentrations of samples were measured using the absorbance at 260 nm/280 nm. The QuantiTect Reverse Transcription Kit (Qiagen) was used to remove genomic DNA and synthesize cDNA.

qPCR was performed using the Bio-Rad Mini Opticon and the iTaq Universal SYBR Green Supermix (Bio-Rad). Reactions contained the appropriate amounts of reagents as specified by kit protocols. Threshold cycle values were set by StepOne software (Thermo Fisher Scientific) and melting curve analysis following amplification was used to verify the quantity of single PCR products. Primers specific for *PDC1*, *ILV2* and *ACT1* are listed in Supplementary Table 7. The expression level of each gene was normalized to that of *ACT1* from the same samples.

Testing gene expression of OptoEXP in 5-l fermenter and higher cell densities. To test OptoEXP in higher cell density conditions, we inoculated YEZ243 into SC-His medium supplemented with 3% glycerol and 2% ethanol and grew in the dark for 24 h. We then set up a BioFlo120 system with a 5-l bioreactor (Eppendorf, B120110002) and added 2.4 l of SC-His medium supplemented with 3% glycerol and 2% ethanol after autoclaving. The reactor was set to 30 °C, pH of 6.5, and a minimum dissolved oxygen percentage of 40. Blue LED strips (Shenzhen Shinesky Optoelectronics, SMD3528) were wrapped around the reactor, covering 73% of the available bulk surface area of the fermentation (Extended Data Fig. 10a, b). These LED strips emitted light at an intensity of 129 μmoles m^{-2} s^{-1} (with 465 nm max peak spectra) measured in the same condition as the light panels. The reactor was then inoculated to an OD_{600} of 1 and the cells were grown in the dark until an OD_{600} of 15 (maintained by covering the reactor with black fabric). At an OD_{600} of 15, the lights were turned on and samples were taken at an OD_{600} of 16 (1 h after induction), 19 (6 h after induction), 41 (24 h after induction), 46 (32 h after induction) and 50 (40 h after induction). Cells were fixed by diluting them to an OD_{600} of 1 in SC-His medium with 3% glycerol and 2% ethanol, adding paraformaldehyde to 3.7%, and incubating for 1 h at 25 °C. To prepare samples for flow cytometry, cells were washed twice with Dulbecco's PBS, and re-suspended again in Dulbecco's PBS to an OD_{600} of 0.5.

Statistics. Statistical significance was determined using a standard *t*-test for *P* values. *T* scores were calculated by the formula: $\frac{(\text{mean}_{\text{condition 2}} - \text{mean}_{\text{condition 1}})\sqrt{\text{number of samples}}}{\text{s.d.}_{\text{condition 2}}}$. *P* values were calculated using a degree of freedom of 2 and a one-sided *t*-test calculator.

Data availability. The authors declare that all data supporting the findings of this study are available within the paper (and its Supplementary Information files), but original data that supports the findings are available from the corresponding authors upon reasonable request.

32. Liu, X. *et al.* Structure-guided engineering of *Lactococcus lactis* alcohol dehydrogenase LlAdhA for improved conversion of isobutyraldehyde to isobutanol. *J. Biotechnol.* **164,** 188–195
33. Lee, J. J., Crook, N., Sun, J. & Alper, H. S. Improvement of lactic acid production in *Saccharomyces cerevisiae* by a deletion of ssb1. *J. Ind. Microbiol. Biotechnol.* **43,** 87–96 (2016).
34. Lee, J. Y., Kang, C. D., Lee, S. H., Park, Y. K. & Cho, K. M. Engineering cellular redox balance in *Saccharomyces cerevisiae* for improved production of L-lactic acid. *Biotechnol. Bioeng.* **112,** 751–758 (2015).
35. Gibson, D. G. *et al.* Enzymatic assembly of DNA molecules up to several hundred kilobases. *Nat. Methods* **6,** 343–345 (2009).
36. Youk, H. & Lim, W. A. Secreting and sensing the same molecule allows cells to achieve versatile social behaviors. *Science* **343,** 1242782 (2014).
37. Chee, M. K. & Haase, S. B. New and redesigned pRS plasmid shuttle vectors for genetic manipulation of *Saccharomyces cerevisiae*. *G3 (Bethesda)* **2,** 515–526 (2012).
38. Yuan, J. & Ching, C. B. Combinatorial assembly of large biochemical pathways into yeast chromosomes for improved production of value-added compounds. *ACS Synth. Biol.* **4,** 23–31 (2015).
39. Goldstein, A. L. & McCusker, J. H. Three new dominant drug resistance cassettes for gene disruption in *Saccharomyces cerevisiae*. *Yeast* **15,** 1541–1553 (1999).
40. Güldener, U., Heck, S., Fielder, T., Beinhauer, J. & Hegemann, J. H. A new efficient gene disruption cassette for repeated use in budding yeast. *Nucleic Acids Res.* **24,** 2519–2524 (1996).
41. Gueldener, U., Heinisch, J., Koehler, G. J., Voss, D. & Hegemann, J. H. A second set of loxP marker cassettes for Cre-mediated multiple gene knockouts in budding yeast. *Nucleic Acids Res.* **30,** e23 (2002).
42. Jones, E. W. & Fink, G. R. in *The Molecular Biology of the Yeast Saccharomyces: Metabolism and Gene Expression* (eds Strathern, J. N. *et al.*) 181–299 (Cold Spring Harbor, 1982).
43. Kern, S. E., Price-Whelan, A. & Newman, D. K. Extraction and measurement of $NAD(P)^+$ and NAD(P)H. *Methods Mol. Biol.* **1149,** 311–323 (2014).
44. Ziv, N., Brandt, N. J. & Gresham, D. The use of chemostats in microbial systems biology. *J. Vis. Exp.* **80,** e50168 (2013).
45. Collart, M. A. & Oliviero, S. Preparation of yeast RNA. *Curr. Protoc. Mol. Biol.* **Chapter 13,** 12 (2001).

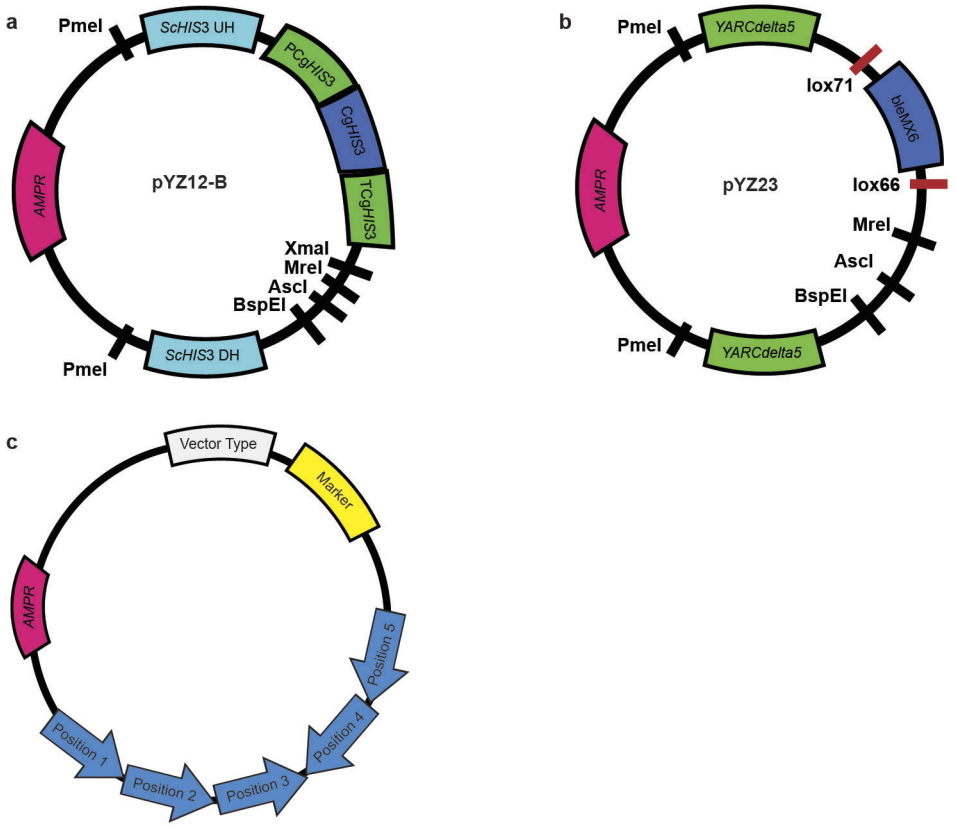

Extended Data Figure 1 | Maps of key vectors used in this study. **a**, pYZ12-B vector used to integrate genes or circuits into the *HIS3* locus. Constructs are usually transferred from pJLA vectors using XmaI and AscI sites. Final constructs are linearized with PmeI before yeast transformation. **b**, pYZ23 vector used to integrate genes or circuits into δ-5 sites of yeast. Constructs are usually transferred from pJLA vectors using MreI and AscI sites. Final constructs are linearized with PmeI before yeast transformation. **c**, The general vector map shows the relative orientation of the five positions listed in Supplementary Table 1, in which different genes (including promoters and terminators) were assembled, using a previously described multiple gene insertion strategy[25]. All vectors have an ampicillin-resistance marker (*AMPR*) for cloning in *E. coli* and a selection marker for *S. cerevisiae* (Marker). Vector types include CEN/ARS, 2μ, or integrative[36–39].

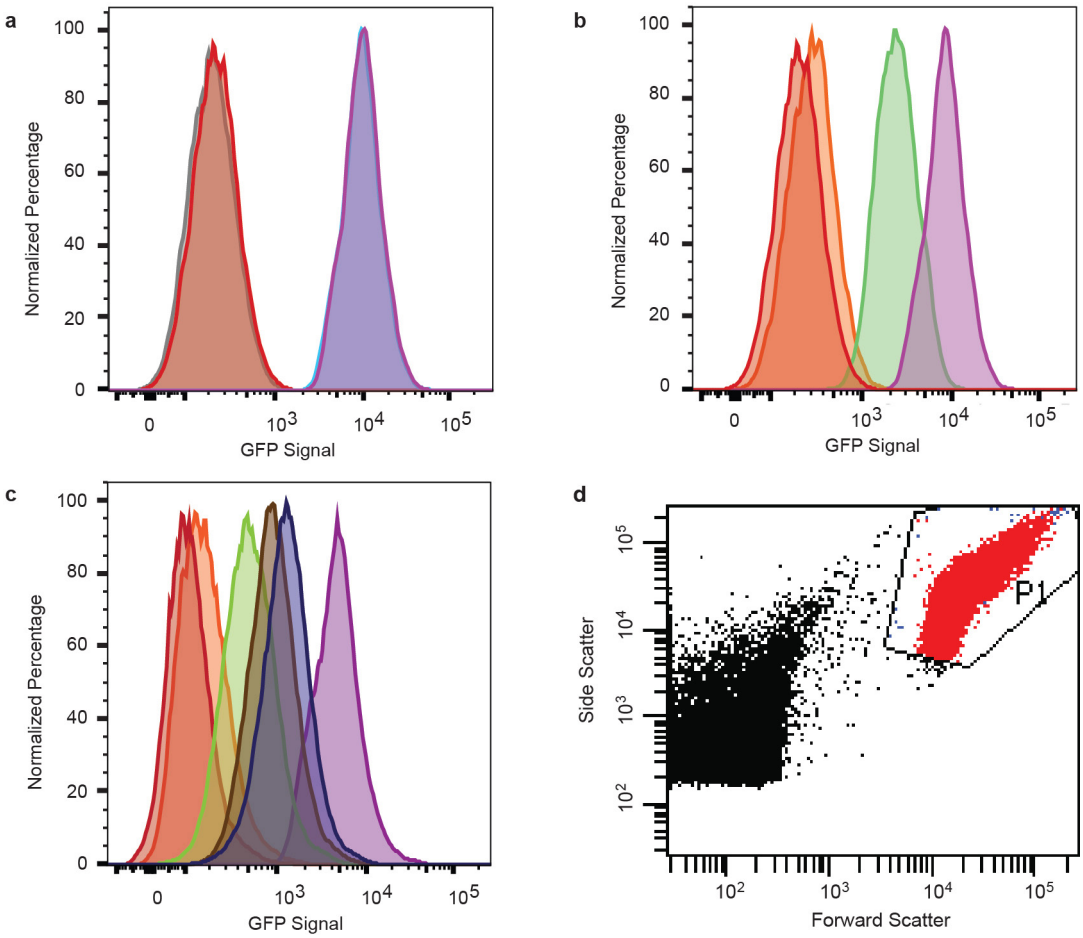

Extended Data Figure 2 | Flow cytometry of strain with GFP controlled by OptoEXP. Representative flow cytometry graphs from three biological replicates under the same conditions. Experiments were performed in 24-well plates, in either glucose or glycerol and ethanol. Every graph is generated from 20,000 cells. **a**, Control strain (YEZ186) with GFP under P_{TEF1} exposed for 3 h to constant blue light (magenta) or kept for the same amount of time in the dark (cyan); these samples are almost completely superimposed on the right-hand side of graph. Control strain (YEZ140) with no GFP exposed for 3 h of constant blue light (red) or kept for the same amount of time in the dark (grey); these samples are almost completely superimposed on the left-hand side of graph. Under these conditions, there is no detectable photobleaching. **b**, Light-induced GFP expression in YEZ139, a strain with GFP controlled by OptoEXP. GFP expression in YEZ139 in SC-His medium supplemented with 2% glucose after 3 h of exposure to blue light (green) is homogeneous across the cell population, and 37-fold higher than in YEZ139 cells kept in the dark for the same amount of time (orange). The maximum level of GFP expression obtained by OptoEXP in YEZ139 grown in full light for 3 h (green) is 22.1% of what is achieved in YEZ186, which contains P_{TEF1}–GFP, grown under the same conditions (magenta). Fluorescence from a control wild-type strain without GFP, YEZ140, grown for 3 h in the light, is shown for comparison (red). **c**, Light-induced GFP expression by OptoEXP in YEZ243 in SC-His medium supplemented with 3% glycerol and 2% ethanol. Starting from cultures grown in the dark, samples were taken (in the exponential growth phase, at an OD_{600} of approximately 3) and incubated in 24-well plates under the following light conditions: 2 h in the dark (orange); 1.5 h in the dark followed by 30 min in light (green); 1 h in the dark, followed by 1 h in light (brown); or 2 h in light (dark blue). YEZ140 (red) and YEZ186 (magenta) were used as controls with no GFP expression and GFP expression from a strong, constitutive promoter (P_{TEF1}), respectively. **d**, Example of the gating used to make the flow cytometry plots in **a**–**c**. All experiments were repeated at least three times.

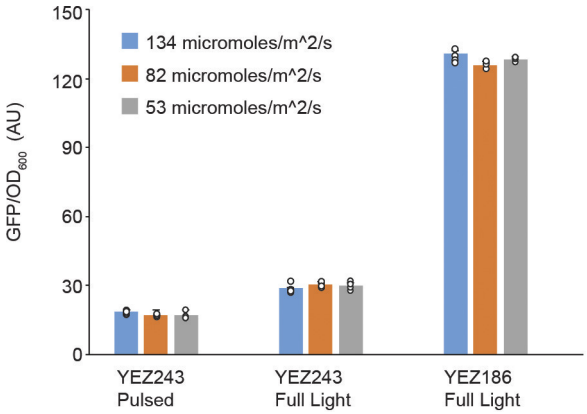

Extended Data Figure 3 | OptoEXP performance under LED panels of different intensities. Light-induced expression of GFP in YEZ243 (OptoEXP driving GFP) compared to constitutive GFP expression in YEZ186 (P_{TEF1}–GFP), using light panels of different intensities. Pulsed light was applied at duty cycles of 10 s on and 70 s off. Data are shown as mean values; dots represent individual data points; error bars represent the s.d. from four biologically independent 1-ml culture sample replicates. All experiments were repeated at least three times.

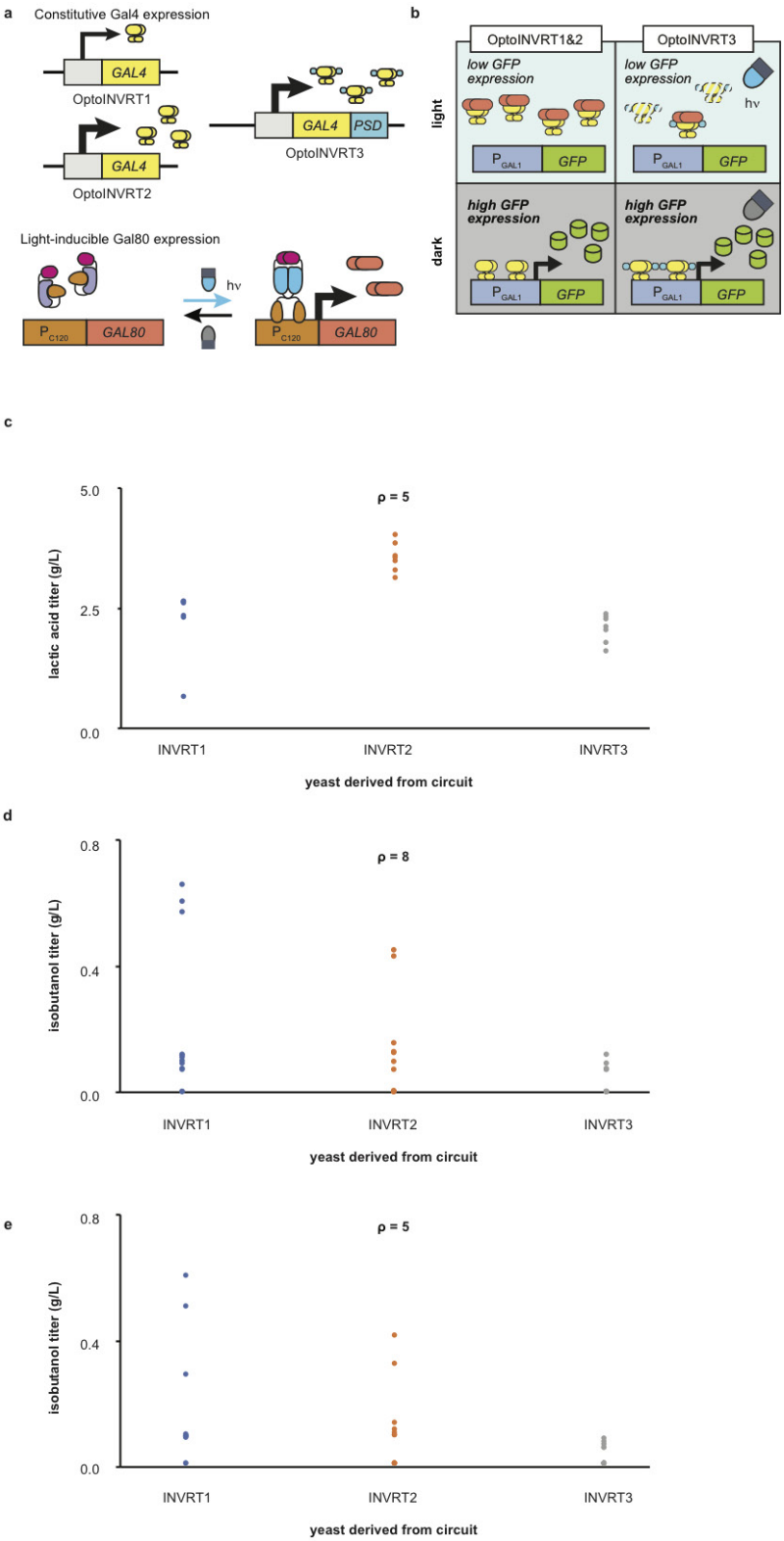

Extended Data Figure 4 | Comparison of OptoINVRT light-repressible transcription circuits. a, OptoINVRT circuit design, based on the expression of Gal80 from OptoEXP and of Gal4 from constitutive promoters of different strength, with or without a PSD domain. **b**, Genes controlled by OptoINVRT circuits are repressed in the light and activated in the dark by the repression activity of Gal80 on Gal4 transcription factor. The PSD fused to Gal4 in OptoINVRT3 stimulates protein degradation in the light. **c**, Screens for lactic acid production in 2% glucose of several colonies of strains YEZ144 (OptoINVRT1), YEZ145 (OptoINVRT2) and YEZ146 (OptoINVRT3), using growth parameters: $\rho = 5$ and $\theta = 6$ h, where ρ is the cell density at which cells are moved from light to dark and θ is the time cells are incubated in the dark before starting the fermentation ($n = 7$ biologically independent colonies). **d**, Screens for isobutanol production in 2% glucose of several colonies of YEZ159 (OptoINVRT1), YEZ156 (OptoINVRT2) and HPY6 (OptoINVRT3), using growth parameters: $\rho = 8$ and $\theta = 3$ h ($n = 12$ biologically independent colonies). **e**, Screens for isobutanol production in 2% glucose of several colonies of YEZ159 (OptoINVRT1), YEZ156 (OptoINVRT2) and HPY6 (OptoINVRT3), using growth parameters: $\rho = 5$ and $\theta = 3$ h ($n = 12$ biologically independent colonies). The screens shown in **c**–**e** were performed once in our laboratory.

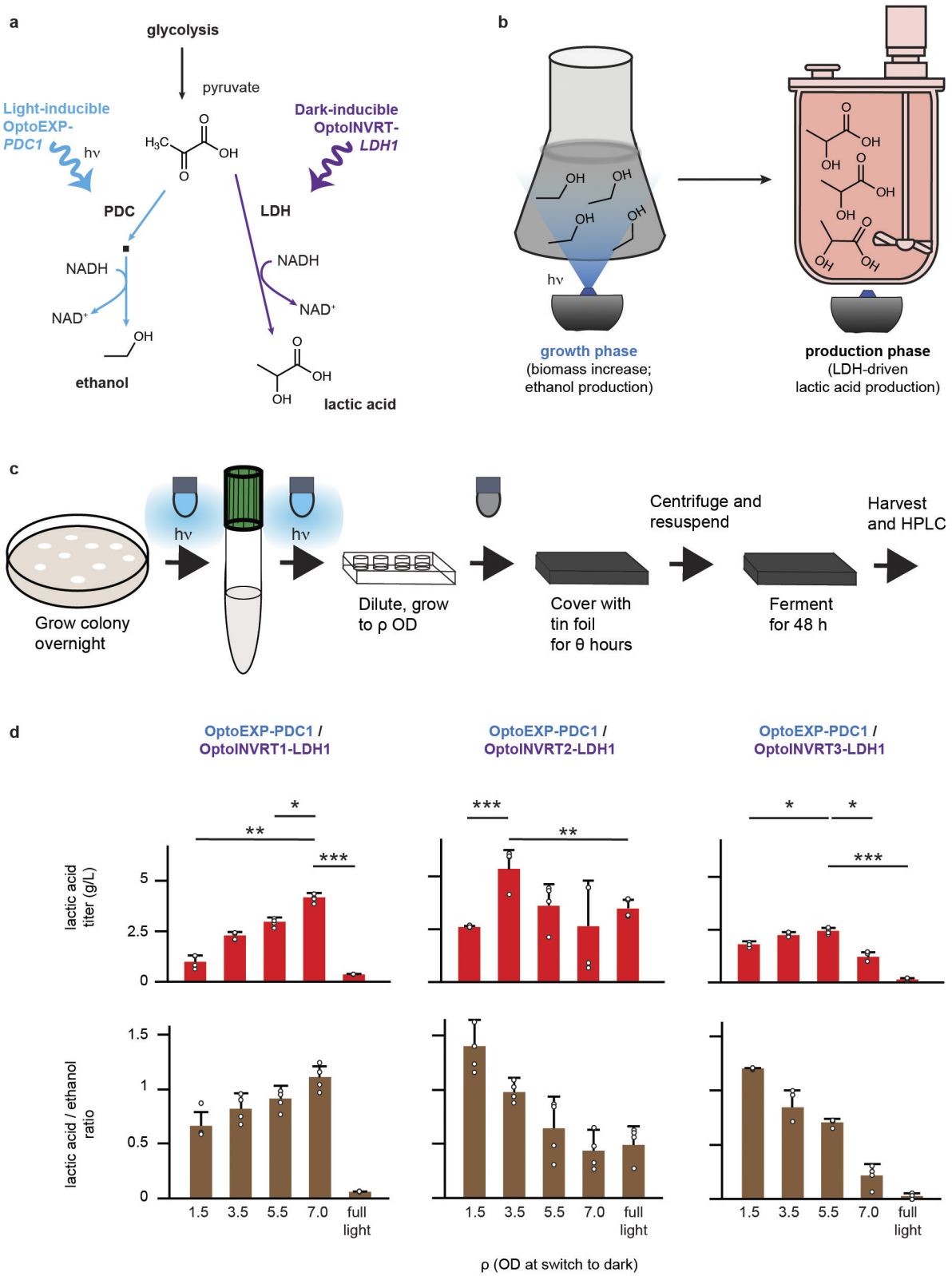

Extended Data Figure 5 | Light-controlled lactic acid production. **a**, Lactic acid is produced by the reduction of pyruvate by Ldh. *PDC1* is controlled by OptoEXP and Ldh by OptoINVRT circuits. **b**, With optogenetic controls, light can be used to separate fermentation into two phases: a growth phase when cultures are exposed to light, during which *PDC1* is expressed and Ldh is repressed, and a lactic acid production phase when cells are in the dark, during which *PDC1* is not induced, and Ldh is expressed. **c**, Experimental design for the screening of strains and optimization of conditions. ρ and θ were varied in these experiments. **d**, Three OptoINVRT circuits were tested for lactic acid production: OptoINVRT1 (YEZ144); OptoINVRT2 (YEZ145) and OptoINVRT3 (YEZ146). Top, dependence of lactic acid titres on ρ. Bottom, dependence of the ratio of lactic acid to ethanol on ρ. Fermentations were done in 26.5 g l^{-1} glucose and run for 2 days. All samples had $\theta = 6$ h. Data are shown as mean values; dots represent individual data points; error bars represent the s.d. of three biologically independent 1-ml culture sample replicates exposed to the same light conditions. $^{*}P < 0.05$, $^{**}P < 0.01$, $^{***}P < 0.001$. Statistics are derived using a one-sided *t*-test. All experiments were repeated at least three times.

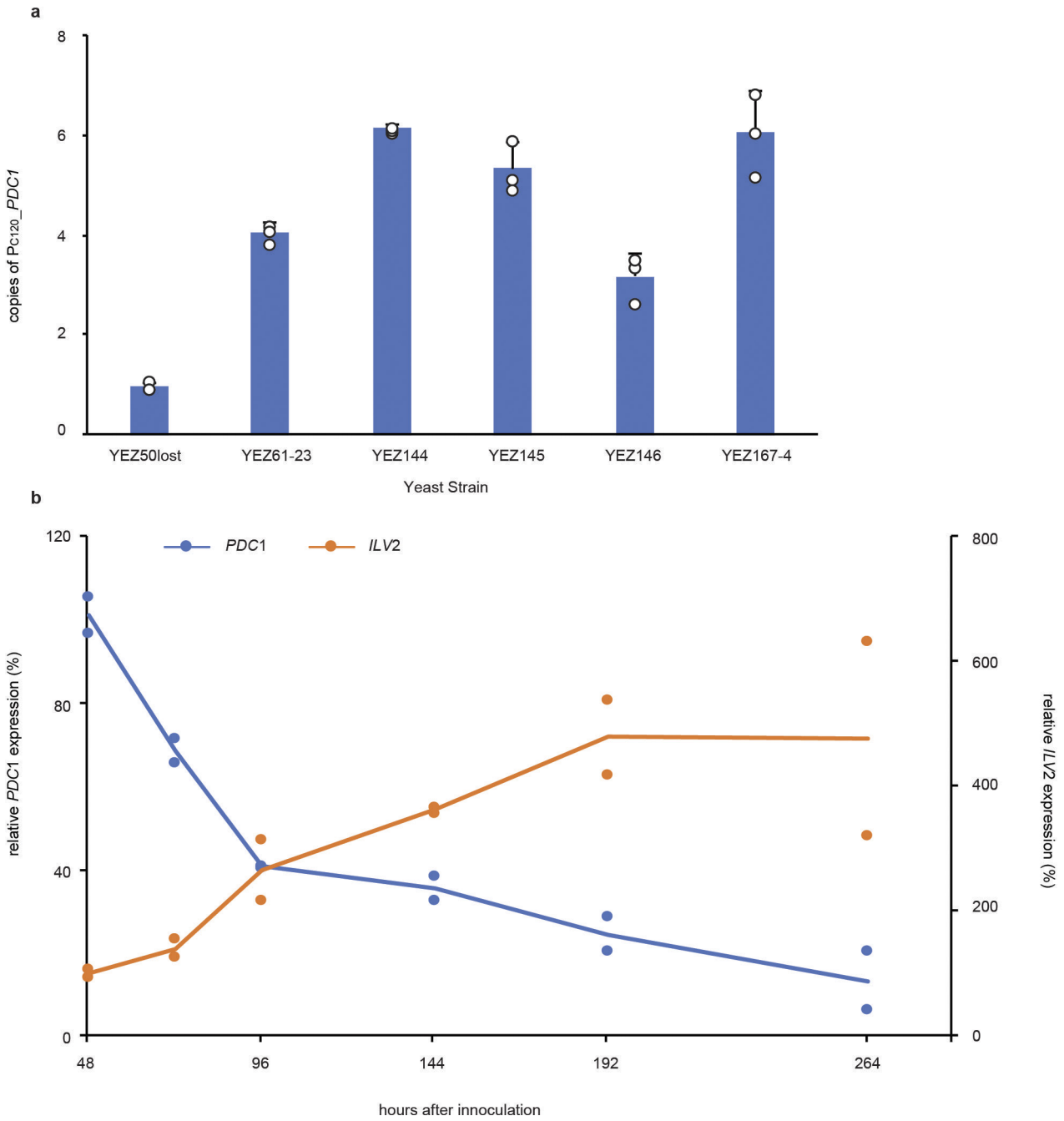

Extended Data Figure 6 | qPCR experiments. a, Number of copies of P_{C120} driving *PDC1* in key strains, determined with qPCR performed on genomic DNA samples (see Methods). All strains have one copy of *PDC1* integrated in the *HIS3* locus, and the rest are integrated in random δ-integration sites (except YEZ50lost, which only has one copy in the *HIS3* locus). Data are shown as mean values; dots represent individual data points; error bars represent the s.d. from three biologically independent 1-ml culture sample replicates. All experiments were repeated at least three times. **b**, qPCR of *PDC1* and *ILV2* mRNA levels during fed-batch fermentation with periodic light stimulation for isobutanol production in 0.5-l fermenters. qPCR was performed on samples from fed-batch fermentations for isobutanol production (Fig. 3e) to measure concentrations of *PDC1* and *ILV2* transcripts. Gene expression was normalized to *ACT1* transcripts. Lines represent average values from samples taken from two biologically independent fermentations run under the same conditions. All experiments were repeated at least two times.

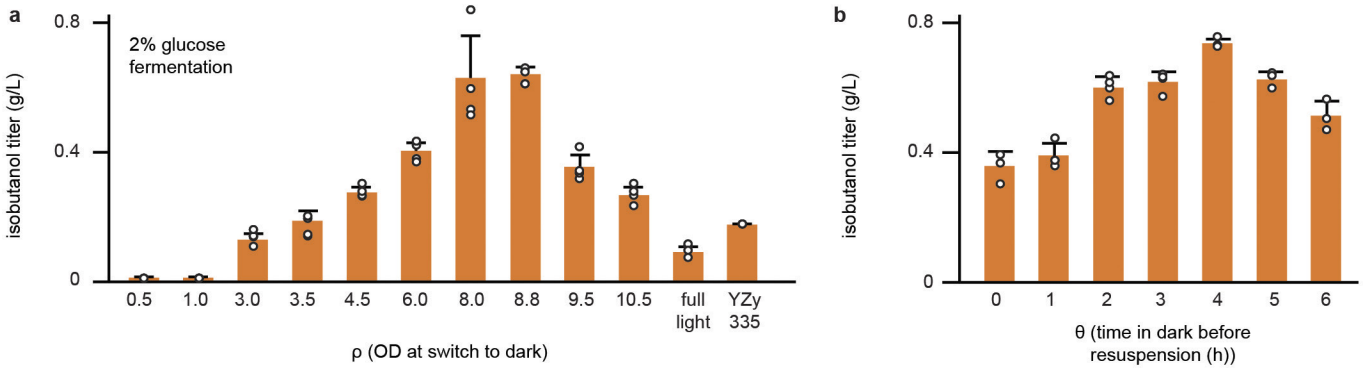

Extended Data Figure 7 | Optimization of light-controlled isobutanol production. a, Dependence of isobutanol titres on ρ. Cells were grown with $\theta = 3$ h; fermentations were done in 21.5 g l^{-1} glucose; isobutanol titres were measured after 2 days of fermentation in the dark. YZy335 is a control strain with a constitutive isobutanol pathway plasmid and wild-type *PDC1*, *PDC5* and *PDC6* and was used in 2-day fermentations at high cell density as a control. **b**, Dependence of isobutanol titres on θ. Cells were grown to $\rho = 8.5$. Fermentations were again done in 20.8 g l^{-1} glucose for 2 days in the dark. All data are shown as mean values; dots represent individual data points; error bars represent the s.d. of three biologically independent 1-ml culture sample replicates exposed to the same light conditions. All experiments were repeated at least three times.

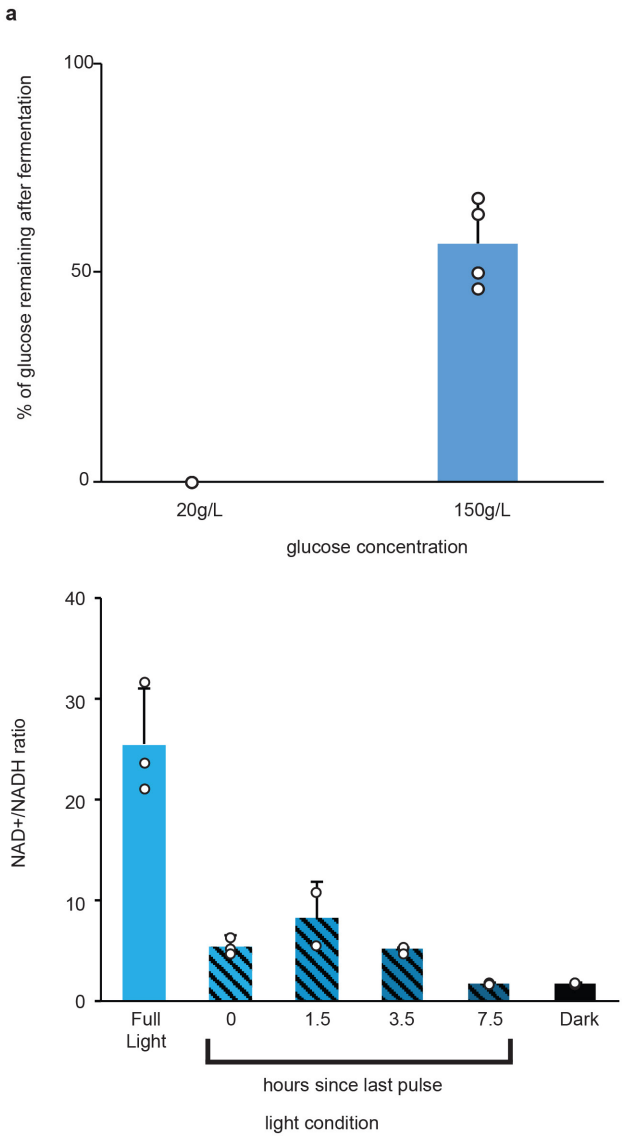

Extended Data Figure 8 | Optimization of high glucose fermentations. **a**, Glucose remainders as a percentage of initial glucose concentration after 48 h (20 g l^{-1} initial glucose) or 80 h (150 g l^{-1} initial glucose) of fermentation of YEZ167-4 in the dark. Cell growth parameters: $\rho = 8.5$ and $\theta = 4$ h (for fermentations in 20 g l^{-1} glucose) and $\rho = 9.5$ and $\theta = 3$ h (for fermentations in 150 g l^{-1} glucose). Data are shown as mean values; dots represent individual data points; error bars represent the s.d. from three biologically independent 1-ml culture sample replicates. All experiments were repeated at least three times. **b**, NAD^+/NADH ratio recovery through light pulsing. NAD^+/NADH ratios were measured in samples under similar batch fermentation conditions as shown in Fig. 3c (see Methods). YEZ167-4 cultures were diluted into six 24-well plates and grown to an OD_{600} of 9.5 and left in the dark for 3 h before resuspending cells in 15% glucose medium. Four of the plates were pulsed every 10 h for 30 min at a duty cycle of 15 s on and 65 s off. Cells were harvested after 48-h fermentations, and at different times after the last light pulse (0, 1.5, 3.5, or 7.5 h). Control plates were kept under full light or in the dark throughout the 48-h fermentations. NAD^+/NADH ratios in pelleted cells were measured following a previously described method[43]. Data are shown as mean values; dots represent individual data points; error bars represent the s.d. of four biologically independent 1-ml culture sample replicates. All experiments were repeated at least three times.

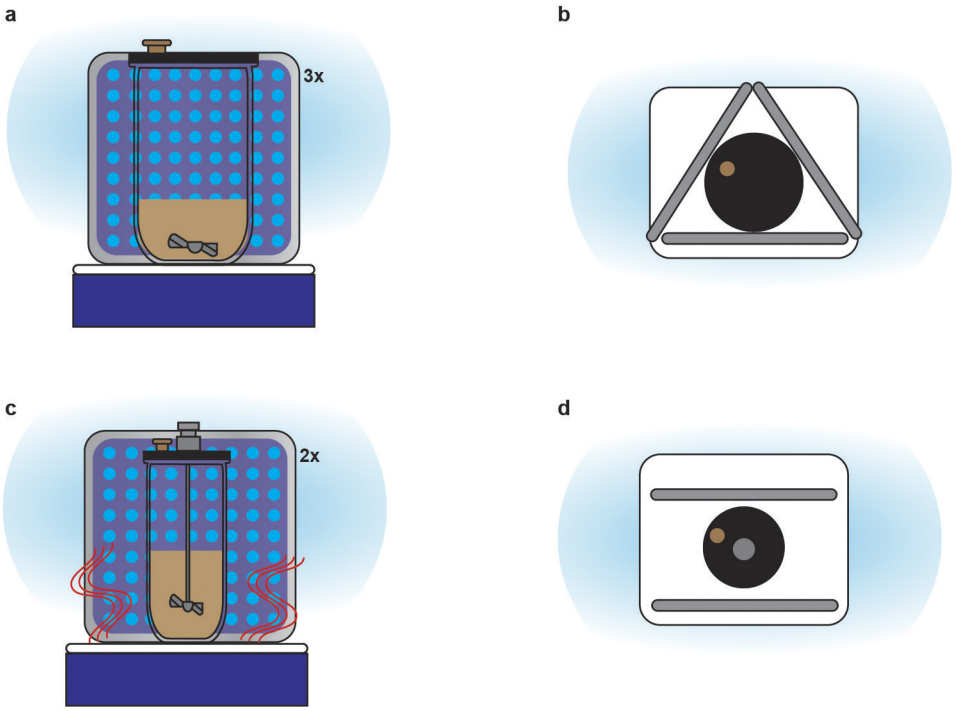

Extended Data Figure 9 | Diagrams of light-stimulated laboratory-scale fermenters used to test YEZ167-4. a, **b**, The 2-l bioreactor was set up so that three light panels could be placed around the fermenter. A magnetic stir plate and stir bar were used to mix the culture, and fermentations were performed in a 30 °C warm-room. **c**, **d**, The 500-ml fed-batch bioreactor was set up so that two light panels could be placed around the fermenter. The culture was mixed with a motorized propeller and a heat plate with temperature control probe was used to maintain the temperature at 30 °C.

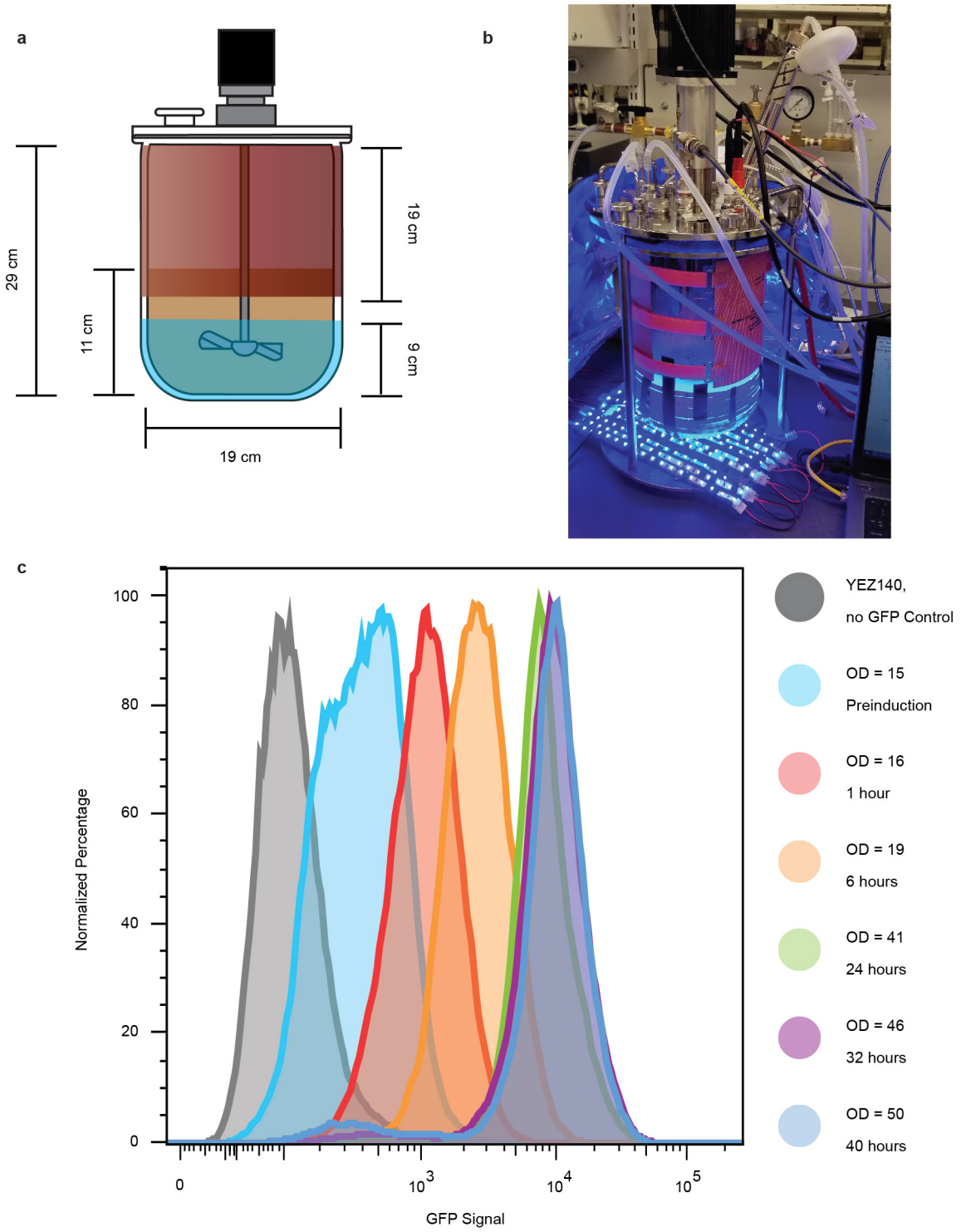

Extended Data Figure 10 | Light-dependent GFP expression in laboratory-scale fermenter at relatively high cell densities. a, Schematic of 5-l fermenter setup with the dimensions of the area exposed to light. Red is the heating blanket around the reactor. Brown depicts the cell culture (2.5 l). Blue depicts the area being illuminated by blue LEDs. **b**, Picture of the functioning 5-l, light-stimulated fermenter. **c**, Representative flow cytometry results from two fermentation replicates using YEZ243, which has light-inducible GFP expression. Cells were grown in fed-batch mode using a glycerol feed to achieve the highest cell densities possible in this setup. Yeast cells were exposed to light when they reached an OD_{600} of 15 and left under continuous illumination for the rest of the experiment. Samples from the fermenter were fixed at the time of harvesting to prevent time-dependent variations. Grey was a sample of YEZ140 without GFP, which was used as a control. Light blue is pre-induction at an OD_{600} of 15; red is after 1 h of induction at an OD_{600} of 16; orange is after 6 h of induction at an OD_{600} of 19; green is after 24 h of induction at an OD_{600} of 41; purple is after 32 h of induction at an OD_{600} of 46 and dark blue is after 40 h of induction at an OD_{600} of 50. Every curve is generated from 20,000 cell counts. Data from the other fermenter run, which are very similar, are available upon request. All experiments were repeated at least three times.

Corresponding author(s): Jose L. Avalos, Jared E. Toettcher

Life Sciences Reporting Summary

Nature Research wishes to improve the reproducibility of the work that we publish. This form is intended for publication with all accepted life science papers and provides structure for consistency and transparency in reporting. Every life science submission will use this form; some list items might not apply to an individual manuscript, but all fields must be completed for clarity.

For further information on the points included in this form, see Reporting Life Sciences Research. For further information on Nature Research policies, including our data availability policy, see Authors & Referees and the Editorial Policy Checklist.

Please do not complete any field with "not applicable" or n/a. Refer to the help text for what text to use if an item is not relevant to your study.
For final submission: please carefully check your responses for accuracy; you will not be able to make changes later.

Experimental design

1. Sample size

   Describe how sample size was determined.

   Samples sizes of n >= 3 (except a long 5-L photobioreactor experiment in which n = 2) were measured so that p-values calculated from a standard t-test would yield a one-tail probably of lower than 0.05. The only experiment where the sample size was equal to two was for a high cell density growth experiment in a 5-L fermenter that took substantial time and effort to set up and run. However, the standard error between measurements in these experiments did not exceed 4.8% and the statistical significance of increased gene induction at the highest cell density has p = 9.2 E-11, considering that our flow cytometry measurements were done on 20,000 cells for each run.

2. Data exclusions

   Describe any data exclusions.

   We did not exclude any data

3. Replication

   Describe the measures taken to verify the reproducibility of the experimental findings.

   All experimental findings are reliably reproducible. We have reproduced each experiment at least twice to ensure reliability, and have encountered no problems with reproducibility

4. Randomization

   Describe how samples/organisms/participants were allocated into experimental groups.

   All samples in the same experimental group were biological replicates (same genetic makeup but different original colony). We did not need to randomize any experiments because all statistics were done with genetically identical samples.

5. Blinding

   Describe whether the investigators were blinded to group allocation during data collection and/or analysis.

   Investigators were blinded to group allocation for select experiments in which this was possible. For example, in the NAD+/NADH ratio measurements, the fermentation and sample collection was carried out by one researcher (Zhao) and blind NAD+/NADH ratio measurements and analysis were carried out by a different researcher (Zhang). Other sets of experiments, for example the light-dose-dependent growth measurements were reproduced by two different researchers (in this particular case by Zhao and Mehl).

Note: all in vivo studies must report how sample size was determined and whether blinding and randomization were used.

6. Statistical parameters

For all figures and tables that use statistical methods, confirm that the following items are present in relevant figure legends (or in the Methods section if additional space is needed).

n/a	Confirmed
☐	☒ The exact sample size (*n*) for each experimental group/condition, given as a discrete number and unit of measurement (animals, litters, cultures, etc.)
☐	☒ A description of how samples were collected, noting whether measurements were taken from distinct samples or whether the same sample was measured repeatedly
☐	☒ A statement indicating how many times each experiment was replicated
☐	☒ The statistical test(s) used and whether they are one- or two-sided *Only common tests should be described solely by name; describe more complex techniques in the Methods section.*
☐	☒ A description of any assumptions or corrections, such as an adjustment for multiple comparisons
☐	☒ Test values indicating whether an effect is present *Provide confidence intervals or give results of significance tests (e.g. P values) as exact values whenever appropriate and with effect sizes noted.*
☐	☒ A clear description of statistics including central tendency (e.g. median, mean) and variation (e.g. standard deviation, interquartile range)
☐	☒ Clearly defined error bars in all relevant figure captions (with explicit mention of central tendency and variation)

See the web collection on statistics for biologists for further resources and guidance.

Software

Policy information about availability of computer code

7. Software

Describe the software used to analyze the data in this study.

Microsoft Excel, Agilent Chemstation, FlowJo, and StepOne

For manuscripts utilizing custom algorithms or software that are central to the paper but not yet described in the published literature, software must be made available to editors and reviewers upon request. We strongly encourage code deposition in a community repository (e.g. GitHub). *Nature Methods* guidance for providing algorithms and software for publication provides further information on this topic.

Materials and reagents

Policy information about availability of materials

8. Materials availability

Indicate whether there are restrictions on availability of unique materials or if these materials are only available for distribution by a third party.

There are no restrictions on material availability.

9. Antibodies

Describe the antibodies used and how they were validated for use in the system under study (i.e. assay and species).

No Antibodies were used in this study.

10. Eukaryotic cell lines

a. State the source of each eukaryotic cell line used.

Yeast strains BY4741 and CEN.PK2-1C

b. Describe the method of cell line authentication used.

by genotype, and phenotype analysis. Purchased from Euroscarf

c. Report whether the cell lines were tested for mycoplasma contamination.

Cell lines were not tested for mycoplasma contamination.

d. If any of the cell lines used are listed in the database of commonly misidentified cell lines maintained by ICLAC, provide a scientific rationale for their use.

No commonly misidentified cell lines were used in this study.

Animals and human research participants

Policy information about studies involving animals; when reporting animal research, follow the ARRIVE guidelines

11. Description of research animals

Provide all relevant details on animals and/or animal-derived materials used in the study.

No animals were used in this study.

Policy information about studies involving human research participants

12. Description of human research participants

Describe the covariate-relevant population characteristics of the human research participants.	This study did not involve human participants.

nature research

Corresponding author(s): Jose Avalos and Jared Toettcher

☐ Initial submission ☐ Revised version ☒ Final submission

Flow Cytometry Reporting Summary

Form fields will expand as needed. Please do not leave fields blank.

Data presentation

For all flow cytometry data, confirm that:

☒ 1. The axis labels state the marker and fluorochrome used (e.g. CD4-FITC).

☒ 2. The axis scales are clearly visible. Include numbers along axes only for bottom left plot of group (a 'group' is an analysis of identical markers).

☒ 3. All plots are contour plots with outliers or pseudocolor plots.

☒ 4. A numerical value for number of cells or percentage (with statistics) is provided.

Methodological details

5. Describe the sample preparation.	Cells are grown in yeast media and then diluted into PBS solution or fixed with formaldehyde.
6. Identify the instrument used for data collection.	BD LSR II flow cytometer (BD Biosciences, San Jose, CA, USA)
7. Describe the software used to collect and analyze the flow cytometry data.	FlowJo Version 10 software (Tree Star, Ashland, OR, USA)
8. Describe the abundance of the relevant cell populations within post-sort fractions.	Relevant cell fractions were always above 85% for all samples.
9. Describe the gating strategy used.	The gating used in our analyses was defined to include positive (YEZ186) and negative (YEZ140) control cells based on GFP fluorescence, but exclude particles that are either too small or too large to be single living yeast cells, based on the side scatter (SSC-A) vs forward scatter (FSC-A) plots

Tick this box to confirm that a figure exemplifying the gating strategy is provided in the Supplementary Information. ☒